Master's thesis

NTNU
Norwegian University of Science and Technology
Faculty of Natural Sciences
Department of Biotechnology and Food Science

Brynjar Skagestad

Effect of hydrogen peroxide in the production of L-lysine derived amino acids in *Bacillus methanolicus*

Master's thesis in Chemical Engineering and Biotechnology
Supervisor: Luciana Fernandes de Brito
Co-supervisor: Marta Irla
June 2022

NTNU
Norwegian University of Science and Technology

Brynjar Skagestad

Effect of hydrogen peroxide in the production of L-lysine derived amino acids in *Bacillus methanolicus*

Master's thesis in Chemical Engineering and Biotechnology
Supervisor: Luciana Fernandes de Brito
Co-supervisor: Marta Irla
June 2022

Norwegian University of Science and Technology
Faculty of Natural Sciences
Department of Biotechnology and Food Science

NTNU
Norwegian University of
Science and Technology

Preface

This thesis marks the end of my master's in Chemical Engineering and Biotechnology at the Faculty of Natural Sciences, Norwegian University of Science and Technology (NTNU). The thesis was written under supervision by Luciana Fernandes de Brito, with Marta Irla as my cosupervisor.

I found the topic discussed in the thesis very interesting, and I am very thankful to my supervisor Luciana Fernandes de Brito, for all her support, for always being available for help when I needed it, for letting me work on such an exciting topic, and for all her encouragement. I would also like to thank Marta Irla for her supervision the previous semester and for all the help she has provided. Lastly, I would like to thank the Cell Factories group for including me in their group and for their support.

After five years in Trondheim at NTNU, I would also like to thank all the friends I have made along the way for all the great memories I have made.

Abstract

Bacillus methanolicus, a thermophilic, facultative methylotroph bacterium, has recently received increased interest due to its prospects as a sustainable cell factory in industrial biotechnology. It harbors several traits that justify this; it consumes methanol as the sole carbon and energy source and grows in elevated temperatures. Methanol has the potential to replace traditional feedstocks for bacteria in industrial bioproduction. It can be synthesized by syngas, it is fully miscible and not directly coupled with the global food chain. 5-Aminovalerate (5AVA) and L-pipecolic acid (LPA) are L-lysine derivates that might be generated in a single metabolic pathway. LPA is a common chemical intermediate utilized for the production of chemicals, including anesthetic drug ropivacaine and anticancer agent VX710. 5AVA has promising prospects for use in the chemical synthesis of nylon and glutaric acid, among others. In this study, the effect of hydrogen peroxide on the biosynthetic pathway of these compounds, the L-lysine α-oxidase pathway, is tested in *B. methanolicus*. The genes encoding the enzymes involved in the pathway were overexpressed in the organism to obtain the production of LPA and 5AVA. In addition, the enzyme catalase was overexpressed in order to either remove hydrogen peroxide in the case of LPA production or control the concentration of supplemented hydrogen peroxide in the bacterial culture to increase the 5AVA production by decreasing the susceptibility of *B. methanolicus* to the compound. Furthermore, this study found that the toxicity of 5AVA impacted the production of the compound in *B. methanolicus*, and the induction time was found to be important when producing LPA, with later induction times being favored. A titer of 17.14 ± 7.51 mg/l and 21.41 ± 11.72 mg/l was achieved for LPA and 5AVA, respectively.

Oppsummering

Bacillus methanolicus er en termofil, fakultativ metylotrofisk bakterie som nylig har tiltrukket seg økt interesse for sitt potensiale som en bærekraftig cellefabrikk innenfor industriell bioteknologi. Bakteriens evne til å benytte metanol som karbon og energikilde, samt at den er termofil er grunnene til dette. Metanol har potensiale til å erstatte tradisjonelle energikilder i cellekulturer innenfor industriell bioproduksjon. Stoffet kan bli produsert fra syntesegas, det er lett blandbart og stoffer er heller ikke direkte koblet opp mot den globale matvareforskyningen. 5-Aminovalerat (5AVA) og L-pipekolsyre (LPA) er L-lysinderivater, som kan bli syntetisert fra det samme metabolske sporet. LPA er et vanlig kjemisk mellomprodukt som ofte benyttes under produksjonen av høyverdi kjemikalier som anestesimiddelet ropivakain og antikreftmiddelet VX710. 5AVA er et lovende mellomprodukt som kan benyttes under syntesen av blant annet nylon og glutarsyre. I denne studien blir effekten av hydrogenperoksid på biosynteseveien til disse forbindelsene, L-lysin α-oksidase sporet, testet i *B. methanolicus*. Genene som koder for enzymene involvert i dette metabolske sporet ble overuttrykt i organismen for å oppnå produksjon av LPA og 5AVA. I tillegg ble enzymet katalase overuttrykt for enten å fjerne hydrogenperoksid med mål om å øke LPA-produksjonen eller for å øke toleransen til *B. methanolicus* slik at en økt konsentrasjonen av hydrogenperoksid kan tilsettes bakteriekulturen for å øke 5AVA-produksjonen. Videre fant denne studien at toksisiteten til 5AVA påvirket produksjonen av forbindelsen i *B. methanolicus*. Induksjonstiden ble funnet å være viktig ved produksjon av LPA, hvor man fant at induksjon etter fire time gav høyest konsentrasjon av LPA. En konsentrasjon på 17,14 $\pm$ 7,51 mg/l og 21,41 $\pm$ 11,72 mg/l ble oppnådd for henholdsvis LPA og 5AVA.

Contents

Abbreviations

5AVA	5-Aminovalerate
LPA	L-pipecolic acid
HPLC	High performance liquid chromatography
EPB	Electroporation buffer
OD_{600}	Optical density at 600 nm
Lethal concentration 50	LC_{50}
Methanol dehydrogenase	MDH
Ribulose-5-phosphate	R5P
Hexulose-6-phosphate	H6P
Fructose-6-phosphate	F6P
Fructose-1,6-biphosphate	FBP
Glyceraldehyde-3-phosphate	G3P
Dihydroxyacetone phosphate	DAHP
Tricarboxylic cycle	TCA
Δ^1-piperideine-6-carboxylate	P2C
L-lysine α-oxidase	AiP
Δ^1-piperideine-6-carboxylate reductase	DpkA
Tris-Acetate-EDTA	TAE

1 Introduction

1.1 *Bacillus methanolicus*: a thermotolerant, methylotrophic platform strain for industrial bioproduction

Bacillus methanolicus, first isolated in 1990, is a rod-shaped, Gram-positive bacterium from the genus *Bacillus*.[1] *B. methanolicus* is a thermophilic methylotroph that can grow between 35 °C and 60 °C with an optimal growth temperature at 50 °C[2], and is able to utilize methanol as the sole carbon and energy source. *B. methanolicus* is a facultative methylotroph that also grows in mannitol, glucose, and arabitol.[3] In 2014, its complete genome was sequenced,[4] later, the genome-scale transcriptome, proteome, and metabolome have been characterized at the genome scale.[5][6][7] *B. methanolicus* presents several advantageous traits, making it an interesting candidate for industrial application. Cultivation at 50 °C reduces the cooling costs associated with large-scale fermentations and the risk of culture contamination by mesophilic species. Moreover, its ability to utilize methanol is what prompted the scientific interest in this species. A microscopic view of the bacterium is shown in Figure 1.1.

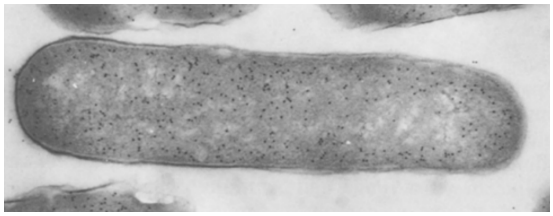

Figure 1.1: Microscopic view of *B. methanolicus*.[8]

B. methanolicus is one of the best-studied methanol-utilizing bacteria. Therefore, it is well suited for further investigation, as the organism is well understood, and multiple genetic tools have been developed to aid in strain engineering. The wild-type strain MGA3 naturally overproduces L-glutamate with titers reaching 59.3 g/l in fed-batch fermentations[9], while classical mutants have been shown to produce 11 g/l L-lysine.[10] Previous metabolic engineering studies in *B. methanolicus* resulted in several different value-added products; a selection of these is shown in Table 1.1.

Table 1.1: *B. methanolicus* production of value-added compounds by the means of metabolic engineering.

Compound	Production [g/L]	Method of cultivation	Reference
Cadaverine	10.2	Fed-batch	[11]
5-Aminovalerate	0.02	Shake-flask	[12]
γ-Aminbutyric acid	9	Fed-batch	[13]
Acetoin	0.42	Shake-flask	[14]
4,4-Diaponeurosporene	Production achieved	Shake-flask	[15]
4,4-Diapolycopene	Production achieved	Shake-flask	[15]

B. methanolicus oxidizes methanol to formaldehyde in a reaction catalyzed by methanol dehydrogenase (MDH).[16] Formaldehyde is then assimilated through the ribulose monophosphate (RuMP) pathway. In this pathway, formaldehyde is fixed with ribulose-5-phosphate (R5P) to form hexulose-6-phosphate (H6P). H6P is then isomerized to create fructose-6-phosphate (F6P). F6P is phosphorylated to fructose-1,6-biphosphate (FBP), and FBP is cleaved to glyceraldehyde-3-phosphate (G3P) and dihydroxyacetone phosphate (DAHP), which is further transformed in a series of reactions to acetyl-CoA that enters tricarboxylic (TCA) cycle where energy is generated. R5P, which initially assimilates formaldehyde in the cycle, is then

regenerated.[17] The methanol assimilation process in *B. methanolicus* is displayed in Figure 1.2.

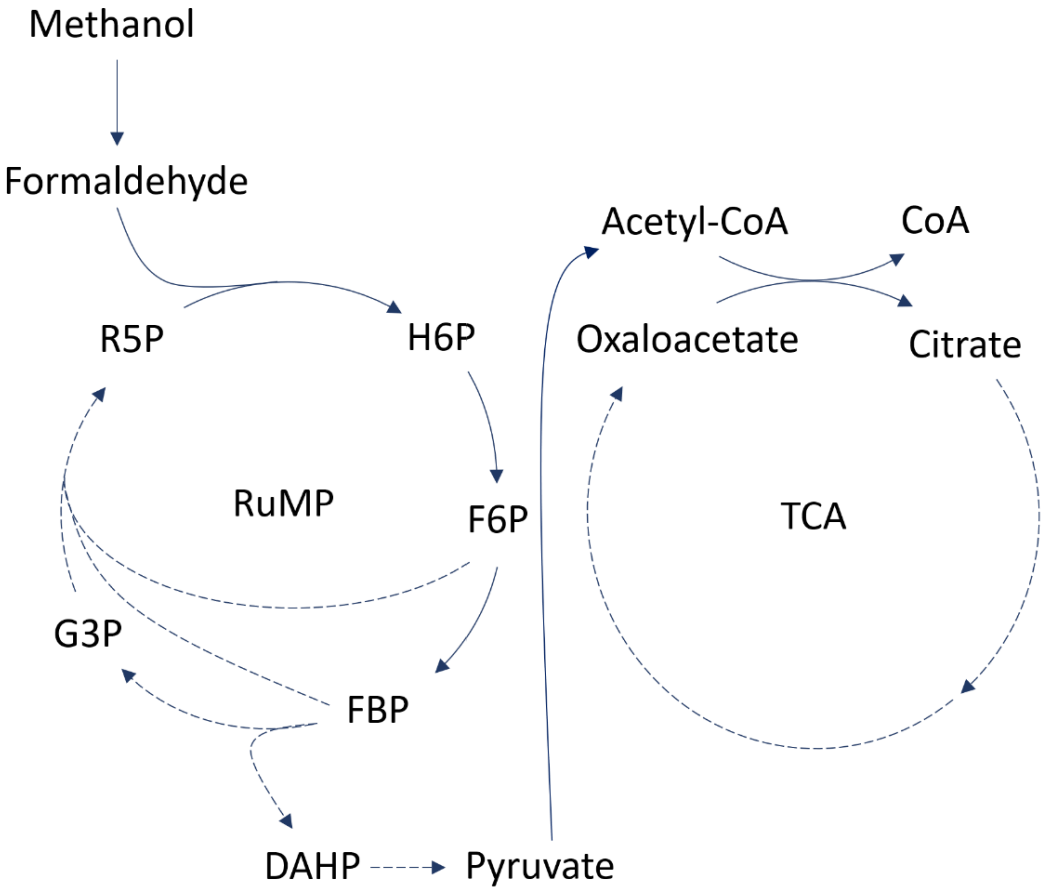

Figure 1.2: Schematic view of the RuMP pathway utilized by microbes oxidizing methanol and its connection to the tricarboxylic (TCA) cycle. This is the pathway for assimilation of methanol in *B. methanolicus*. Dashed lines indicate that multiple enzymatic steps are part of the reaction, while solid lines indicate that only one step is involved. R5P - ribulose-5-phosphate, H6P - hexulose-6-phosphate, F6P - fructose-6-phosphate, FBP - fructose-1,6-biphosphate, G3P - glyceraldehyde-3-phosphate, DAHP - dihydroxyacetone phosphate, CoA - coenzyme A.

1.2 Genetic toolbox of *B. methanolicus*

Despite being one of the best-studied methylotrophic bacteria, *B. methanolicus* still has a limited set of genetic tools available. The lack of genetic tools is one of the major reasons this species has yet to be domesticated for industrial use.[18] Due to the limited availability of genetic tools for the species, the development of novel genetic tools remains a large priority.

A rolling-circle replicating plasmid (pTH1mp) and a theta replicating plasmid (pBV2mp) have previously been established for recombinant gene expression in the species.[4] In addition, the methanol- and mannitol-inducible promoters have been established for plasmid-based gene expression in *B. methanolicus*.[19] For control of gene expression by induction, the heterologous xylose expression system originating in *Bacillus megaterium* has been adapted for the organism.[4] Moreover, the CRISPRi/dCa9 system for gene repression has recently been established in *B. methanolicus*, allowing for the repression of target genes in this bacterium.[20] The CRISPRi/dCa9 system in question was applied to *B. methanolicus*, attempting to repress the *katA* gene, resulting in a 25 % reduction in catalase activity.

1.3 Methanol as a feedstock for industrial biotechnology

Molasses and other agricultural products are the feedstocks most commonly utilized to feed bacterial fermentors. As these feedstocks are coupled with the global food supply, their utilization in industrial biotechnology might increase worldwide food prices and threaten global food security. In addition, increased application of these feedstocks can put pressure on local ecosystems. [18]

Methanol is a one-carbon (C_1) compound not directly utilized in human food production and is therefore considered a promising substitute for the aforementioned feedstocks. It is cheap to produce, easy to transport, and completely miscible. It is also possible to produce methanol from carbon dioxide and hydrogen [18], making it a possible sink for carbon released as CO_2 in the atmosphere. Hydrogen gas can be manufactured without emissions through electrolysis, making methanol production potentially emission-free. Methanol, however, is more reduced than sugars, meaning that bacterial cultures utilizing it as a carbon source require a comparatively higher oxygen supply. [5] This also increases heat production, reducing the cooling cost for methanol-based fermentors, as it is easier to establish a higher ΔT with the cooling media. Methanol also has the advantage of having a comparatively high carbon yield for biomass production of 62 %, [21] compared to glucose at 45 %, [22] requiring less carbon per g of cell mass produced.

1.4 The L-lysine derivatives L-pipecolic acid and 5-aminovalerate

Currently, the demand for amino acids is rapidly increasing, [23] creating a need to increase the production of these compounds. Furthermore, it is estimated that the market for biotechnological products will grow 15.83 % annually from 2021 to 2028. [24] Since the demand for biotechnological products is increasing rapidly, the production of chemicals by bacterial cultivation can be considered relatively economically safe, as long a sufficiently low cost of production is reached.

1.4.1 5-Aminovalerate

5-Aminovalerate (5AVA) is an important 5-carbon non-proteogenic amino acid. 5AVA has recently drawn attention to the possible use case of nylon synthesis. [25] It is also a promising precursor for the synthesis of other 5-carbon platform chemicals, such as glutaric acid, 1,5-pentanediol, and 5-hydroxyvaleric acid. [12]. The chemical structure of the compound is shown in Figure 1.3.

At least five metabolic pathways (both natural and synthetic) have been shown to convert L-lysine to 5AVA in bacteria: The DavBa-pathway, the L-lysine α-oxidase pathway, the SpuI pathway, the PatA pathway, and the Pou pathway. [12] The DavBA converts L-lysine to 5AVA by lysine 2-monooxygenase (DavB) and then 5-aminovaleramidase (DavA). In the L-lysine α-oxidase pathway, L-lysine is deaminated to form α-ketolysine, which is then spontaneously decarboxylated in the prescence of hydrogen peroxide. The three other pathways all start with the decarboxylation of L-lysine to cadaverine by lysine decarboxylase (CadA), which can then enter different patways through activity of either glutamylpolyamine synthetase (SpuI), putrescine aminase (PatA) or putrescine oxidase (Puo), followed by several other enzymatic steps.

The highest titer achieved to date of 5AVA was 240.70 g/l, this was achieved utilizing recombinant *E. coli* overexpressing *davAB* genes originating from *Pseudomonas putida* in a whole-cell biocatalyst system with supplementation of L-lysine with glucose as carbon source. [26] In *B. methanolicus*, 5AVA has been produced to a titer of 0.02 g/l through overexpressing both the PatA pathway and the L-lysine α-oxidase pathway, separately. [12] The same study also tested the three other metabolic pathways for the production of 5AVA previously described, but the recombinant *B. methanolicus* strains overexpressing the pathways were unable to produce 5AVA. Furthermore, 5AVA has been shown to be toxic to *B. methanolicus*, impairing the

growth of the organism at a concentration of 1.17 g/l.[27] The same study utilized adaptive laboratory evolution to establish a strain that achieved a two-fold increase in the maximum cell density compared to the wild-type strain under inhibition by 5AVA.

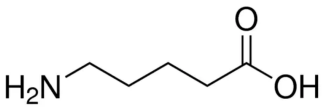

Figure 1.3: Structure formula of 5AVA.[28]

1.4.2 L-Pipecolic acid

L-Pipecolic acid (LPA) is a non-proteinogenic amino acid, and its chemical structure is shown in Figure 1.4. The compound is a chiral intermediate; industrial uses include manufacturing anesthetic drugs such as ropivacaine and bupivacaine, the anticancer agent VX710 and the antibiotic demethoxyrapamycin. Due to the complex production processes and low yields, traditional techniques for synthesizing LPA are considered overly expensive.[29] Therefore, as this chemical is already involved in the metabolism of L-lysine, biosynthesis of the product is a possible alternative.

There exists at least four known enzymatic pathways to produce LPA from L-lysine. The first one, the L-lysine α-oxidase pathway; converts L-lysine to α-ketolysine by L-lysine α-oxidse (encoded by *aiP*) followed by spontaneous conversion to Δ^1-piperideine-2-carboxylate with subsequent activity of Δ^1-piperideine-2-carboxylate reductase (DpkA) to form LPA. The second one, the L-lysine cyclodeamination pathway directly deaminates L-lysine to form LPA by means of L-lysine cyclodeaminase (encoded by *pipA*) activity. The third one, the Δ^1-piperideine-6-carboxylate pathway converts L-lysine to saccharopine, which in turn is converted to Δ^1-piperideine-6-carboxylate through oxidative cleavage by saccharopine oxidase. This compound is then turned into LPA by pyrroline-5-carboxylate reductase (encoded by *proC*).[30] The last pathway, the α-aminoadipic pathway, first converts L-lysine into α-aminoadipic acid, which in turn is converted into LPA.[31]

The highest achieved titer of LPA to date is 61 $\pm$ 3.4 g/l.[32] This was done utilizing recombinant *E. coli*, heterologously overexpressing the L-lysine cyclodeamination pathway. The same study also synthetically regulated the *lysP* and *lysO* genes associated with L-lysine regulation to increase the concentration of L-lysine. In another study LPA was produced in *Corynebacterium glutamicum* with a titer of 0.04 g/l.[33] To the authors' knowledge, LPA production in *B. methanolicus* has yet to be attempted.

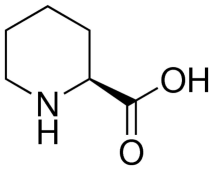

Figure 1.4: Structure formula of LPA.[34]

1.5 The L-lysine α-oxidase pathway for degradation of L-lysine

The conversion of L-lysine by the L-lysine α-oxidase pathway leads to the production of either LPA or 5AVA. This pathway is shown in Figure 1.5. This metabolic pathway starts with the deamination of L-lysine by L-lysine α-oxidase (AiP) to produce α-ketolysine. Notably, this enzymatic step creates hydrogen peroxide as a byproduct. In the second step of the pathway α-ketolysine is either spontaneously decarboxylated to form 5AVA in the presence of hydrogen peroxide, or, in the absence of hydrogen peroxide α-ketolysine is spontaneously dehydrated to

form Δ^1-piperideine-2-carboxylate (P2C). P2C is then reduced to LPA by Δ^1-piperideine-2-carboxylate reductase (DpkA).[35] It has previously been shown that catalase activity increases the production of LPA, as it removes hydrogen peroxide created by the first enzymatic step, hindering the reaction towards 5AVA.[36]

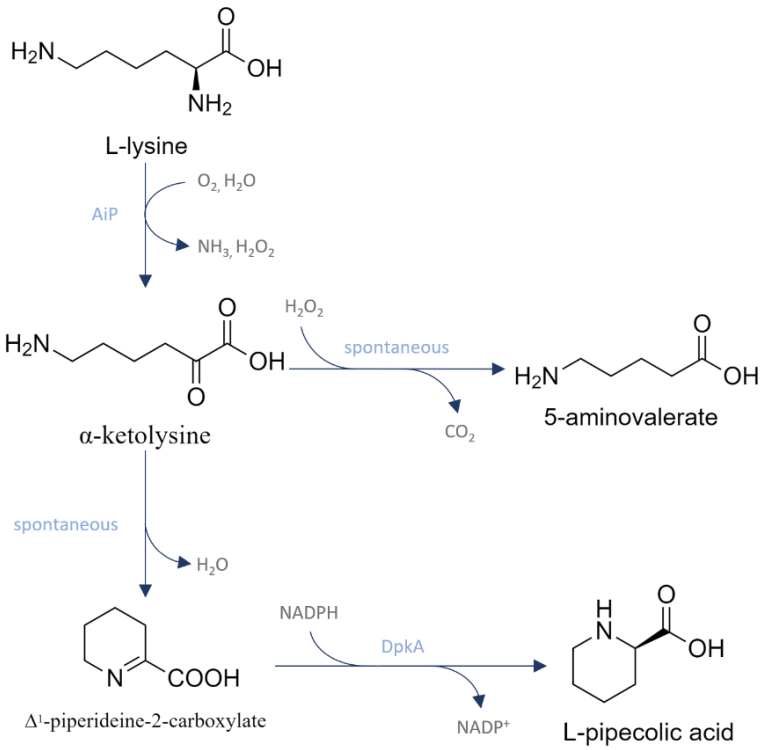

Figure 1.5: Schematic view of the L-lysine α-oxidase pathway. DpkA - Δ^1-piperideine-2-carboxylate reductase, AiP - L-lysine α-oxidase.

1.5.1 The role of catalase in the production of LPA and 5AVA

Catalase is a common enzyme that can be found in many organisms. Its primary function is the dismutation of hydrogen peroxide to form water and oxygen.[37] Hydrogen peroxide is an extremely reactive compound.[38] It exerts oxidative stress on the organism intracellularly, often leading to cell damage. Catalase is one of the most important enzymes detoxifying the compound and is vital to most cells, as hydrogen peroxide is a common byproduct of cellular respiration.[39] The chemical reaction catalyzed by catalase is shown in Equation 1.1.

$$2\,H_2O_2 \xrightarrow{catalase} 2\,H_2O + O_2 \tag{1.1}$$

Upon the synthesis of LPA and 5AVA, the presence of hydrogen peroxide favors the spontaneous reaction converting α-ketolysine into 5AVA over the reaction producing P2C, which later is converted into LPA. Since the initial reaction catalyzed by L-lysine α-oxidase (Aip) produces hydrogen peroxide as a byproduct, hydrogen peroxide is present when Aip is active. Therefore, the addition of catalase activity should increase the production of LPA, as there will be less hydrogen peroxide reacting with α-ketolysine to form 5AVA. Previously, the overproduction of catalase in *B. methanolicus* has been shown to enable the production of LPA by means of the L-lysine α-oxidase pathway.[40]

Catalase activity decreases the susceptibility of *B. methanolicus* to hydrogen peroxide. This allows for cultivating the organism in environments of higher hydrogen peroxide concentrations. Previously, overexpression of catalase in *B. methanolicus* has shown a 10-fold increase

in hydrogen peroxide tolerance.[41] The increased tolerance to hydrogen peroxide allows for the cultivation of the organism supplemented with higher concentrations of the compound, which can lead to increased conversion of α-ketolysine into 5AVA.

1.6 Aim of study

This study is a continuation of the authors' previous work, named 'Assessing Catalase Activity In Bacillus methanolicus: A Prerequisite for Methanol-Based L-Pipecolic Acid Production'[41], which utilized a vector, pTH1mp-$katA^{Bm}$, to overexpress the homologous catalase encoding gene *katA* in *B. methanolicus*. This resulted in a 10-fold decrease in the susceptibility of *B. methanolicus* to hydrogen peroxide, enabling cultivation at higher hydrogen peroxide concentrations.

The study aims to investigate the influence of hydrogen peroxide in the L-lysine α-oxidase pathway heterologously expressed in methylotrophic host *B. methanolicus*. Furthermore, an attempt to increase production of 5AVA and LPA in *B. methanolicus* will be made through regulation of the activity of the endogenous catalase.

2 Materials and methods

2.1 Bacterial strains and plasmids

The general cloning host utilized in this study was *Escherichia coli* DH5α, while *Bacillus methanolicus* MGA3 was utilized as the expression host (Table 2.1). The recombinant *B. methanolicus* strains used in the study are described in Table 2.2. Plasmids used in this study are presented in Table 2.3.

Table 2.1: Wild-type strains utilized for creating the recombinant strains investigated in this study.

Strain	Application	Reference
B.methanolicus MGA3	Expression host	[2]
E. coli DH5α	General cloning host, *F-thi-1 endA1 hsd*R17(r^-,m^-) *supE44 lacU169* (*80lacZM15*) *recA1 gyrA96 relA1*	[42]

Table 2.2: List of recombinant *B. methanolicus* strains investigated in the present study. An explanation of the function of the different plasmids is found in Table 2.3.

Strain	Abbreviation	Reference
B.methanolicus MGA3(pTH1mp-*katA*)(pBV2xp)	MGA3-*katA*-EV	[40]
B.methanolicus MGA3(pTH1mp-*katA*)(pBV2xp-aip^{Tv})	MGA3-*katA*-*Tv*	This study
B.methanolicus MGA3(pTH1mp-*katA*)(pBV2xp-aip^{Sj})	MGA3-*katA*-*Sj*	This study
B.methanolicus MGA3(pTH1mp-*katA*)(pBV2xp-aip^{SjBi})	MGA3-*katA*-*SjBi*	[40]
B.methanolicus MGA3(pTH1mp-*katA*)(pBV2xp-aip^{Bs})	MGA3-*katA*-*Bs*	[40]
B.methanolicus MGA3(pTH1mp-*katA*)(pBV2xp-aip^{Tv}-$dpkA^{Pp}$)	MGA3-*katA*-*Tv*-*Pp*	[40]
B.methanolicus MGA3(pTH1mp-*katA*)(pBV2xp-aip^{Sj}-$dpkA^{Pp}$)	MGA3-*katA*-*Sj*-*Pp*	[40]
B.methanolicus MGA3(pTH1mp-*katA*)(pBV2xp-aip^{SjBi}-$dpkA^{Pp}$)	MGA3-*katA*-*SjBi*-*Pp*	This study
B.methanolicus MGA3(pTH1mp-*katA*)(pBV2xp-aip^{Bs}-$dpkA^{Pp}$)	MGA3-*katA*-*Bs*-*Pp*	This study
B.methanolicus MGA3(pTH1mp-*katA*)(pBV2xp-aip^{SjBi}-$dpkA^{Ps}$)	MGA3-*katA*-*SjBi*-*Ps*	This study
B.methanolicus MGA3(pTH1mp-*katA*)(pBV2xp-aip^{Bs}-$dpkA^{Ps}$)	MGA3-*katA*-*SjBi*-*Ps*	This study

Table 2.3: List of plasmids investigated in current study.

Plasmid	Description	Reference
pTH1mp	Cm^R, Er^R, pHP13 derived *B.subtilis-E.coli* shuttle vector; containting a multiple cloning site downstream of the mhd promoter	[11]
pTH1mp-$katA^{Bm}$	pTH1mp with *katA* gene from *B.methanolicus* under control of the mdh promoter	[40]
pBV2xp	*KanR*, *bla*, pHCM04 derived plasmid, cantaining a multiple cloning site downstream of the xylose inducible promoter	[14]
pBV2xp-aip^{Tv}	pBV2xp with a *aip*-gene from *Trichoderma viride*[2] inserted under control of the xylose inducible promoter	[12]
pBV2xp-aip^{Sj}	pBV2xp with a *aip*-gene from *Scomber japonicus* [2] inserted under control of the xylose inducible promoter	[12]
pBV2xp-aip^{SjBi}	pBV2xp with a *aip*-gene from *Scomber japonicus* [1] inserted under control of the xylose inducible promoter[1]	[12]
pBV2xp-aip^{Bs}	pBV2xp with a *aip*-gene from *Bacillus simplex*[2] inserted under control of the xylose inducible promoter	[12]
pBV2xp-aip^{Tv}-$dpkA^{Pp}$	pBV2xp with a *aip*-gene from *Trichoderma viride*[2] and a *dpkA* gene from *Pseudomonas putida*[2] inserted under control of the xylose inducible promoter	[40]
pBV2xp-aip^{Sj}-$dpkA^{Pp}$	pBV2xp with a *aip*-gene from *Scomber japonicus*[2] and a *dpkA* gene from *Pseudomonas putida*[2] inserted under control of the xylose inducible promoter	[40]
pBV2xp-aip^{Bs}-$dpkA^{Pp}$	pBV2xp with a *aip*-gene from *Bacillus simplex*[2] and a *dpkA* gene from *Pseudomonas putida*[2] inserted under control of the xylose inducible promoter	[40]
pBV2xp-aip^{Bs}-$dpkA^{Ps}$	pBV2xp with a *aip*-gene from *Bacillus simplex*[2] and a *dpkA* gene from *Psudemonas syringae*[2] inserted under control of the xylose inducible promoter	[40]
pBV2xp-aip^{SjBi}-$dpkA^{Pp}$	pBV2xp with a *aip*-gene from *Scomber japonicus*[1] and a *dpkA* gene from *Pseudomonas putida*[2] inserted under control of the xylose inducible promoter[1]	This study
pBV2xp-aip^{SjBi}-$dpkA^{Ps}$	pBV2xp with a *aip*-gene from *Scomber japonicus*[1] and a *dpkA* gene from *Psudemonas syringae*[2] inserted under control of the xylose inducible promoter[1]	This study

[1.] These genes has been codon optimized utilizing a method developed at the University of Bielefeld.[43]

[2.] These genes has been codon optimized utilizing a method published in Nucleic Acids Reasearch.[44]

2.2 Growth conditions

All recipes for growth medium and solutions used in this project can be found in Section A. Precultures of *E. coli* strains were grown in LB medium at 37°C and 225 rpm with 15 mg/ml chloramphenicol or 50 mg/ml kanamycin when appropriate. *B. methanolicus* strains were grown in MVcMY media (Table A.4), MVcM media (Table A.5) or SOB media (Table A.1) at 50 °C and 200 rpm with 5 mg/ml chloramphenicol or 25 mg/ml kanamycin when necessary. Agar plates were prepared by adding 15 g/l bacterial agar to the SOB-media or LB-media. When in need of induction, 1 % $\frac{w}{v}$ sterilized xylose was added to the bacterial culture. All the growth experiments in this study were performed in triplicates, grown in MVcM medium supplemented with antibiotics or xylose when necessary. For the growth and production experiments, pre-cultures were grown overnight and reinoculated to an optical density at 600 nm (OD_{600}) of 0.2. The OD_{600} was measured every 2 hours, and the mean value for the technical triplicates was then utilized to estimate growth and variance of growth. The bacterial cultures were then grown until they reached a maximum value, and the OD_{600} started to decline. OD_{600} was measured 24 and 26 hours after inoculation the next day.

2.3 Plasmid design

This study utilized the pBV2xp plasmid previously established [14] (Table 2.3) as a vector for recombinant gene expression. The plasmid contains the xylose promoter (P_{xylR}) upstream of a multiple cloning site and a ribosome binding site (RBS), the xylose regulatory gene (*XylR*), and the gene conferring resistance to kanamycin (*knt*). The plasmid is 8,104 base pairs long and is shown in Figure 2.1.

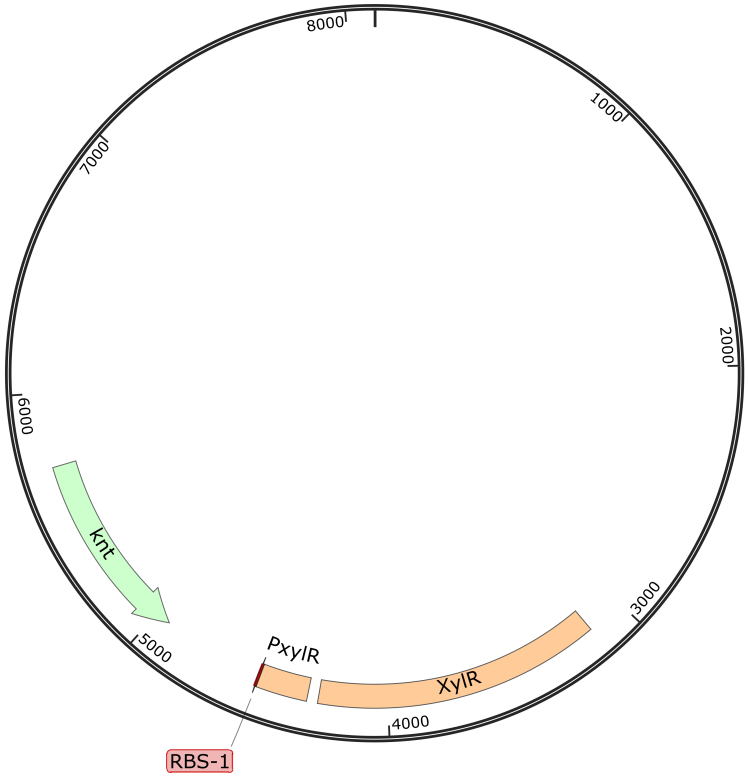

Figure 2.1: Illustration of the pBV2xp plasmid. *knt* indicates kanamycin resistance, (*PxylR*) the xylose promoter, RBS a ribosome binding site and *XylR* indicates the xylose regulatory gene. The multiple cloning site is downstream of the promoter.

In order to enable the production of 5AVA and LPA in *B. methanolicus*, this study targeted the expression of the *aip* gene (for 5AVA production) and the coexpression of *aip* and *dpkA* genes (for LPA production). In both strategies, different gene donors with different genetic backgrounds were tested. The plasmid pBV2xp was used to drive the inducible gene expression. An illustration of a plasmid with a inserted *aip* and one with both *aip* and *dpkA* genes is shown in Figure 2.2. The plasmid was then transformed to *B. methanolicus* for overexpression.

In addition, the plasmid pTH1mp-kat^A was utilized to confer constitutive catalase expression. The plasmid contains a gene conferring chloramphenicol resistance (Cm^R), the methanol dehydrogenase promoter (P_{mdh}), and a gene coding for a catalase enzyme ($katA$). The plasmid pTH1mp-kat^A is sown in Figure 2.3.

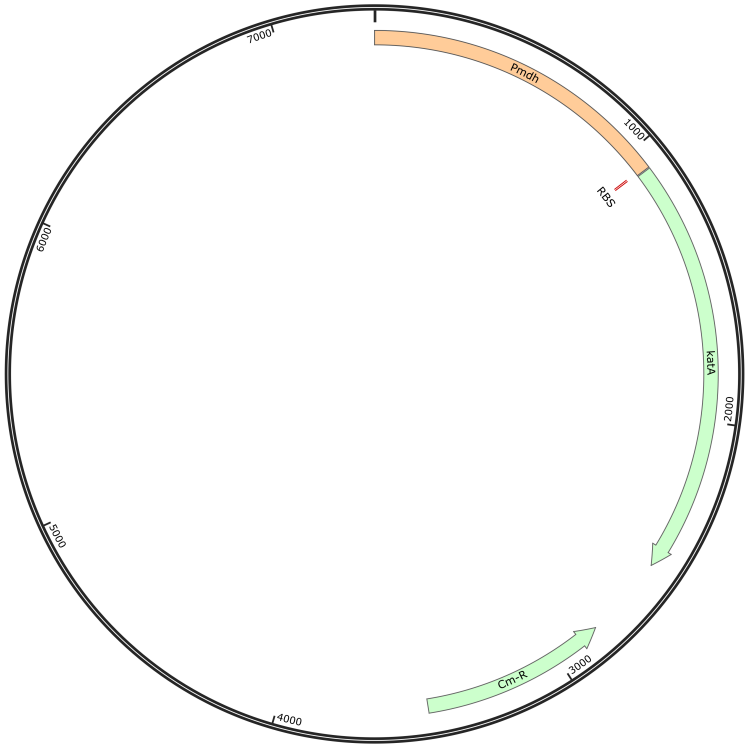

Figure 2.3: Illustration of the pTH1mp-kat^A plasmid. *Cm-R* indicates a gene conferring chloramphenicol resistance, mdh prom the methanol dehydrogenase promotor, and kat^A a gene coding for a catalase enzyme

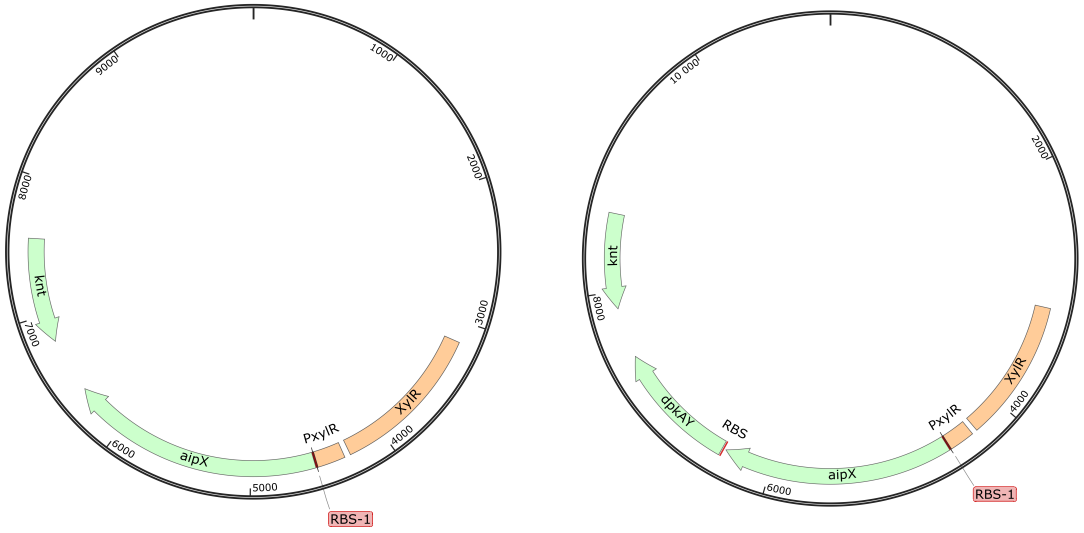

(a) pBV2xp-aip^X **(b)** pBV2xp-aip^X-$dpkA^Y$

Figure 2.2: Illustration of the pBV2xp-aip^X (a) and pBV2xp-aip^X-$dpkA^Y$ (b) plasmids. *knt* indicates a gene conferring kanamycin resistance, (*PxylR*) the xylose promoter, RBS a ribisome binding site, *XylR* the xylose regulatory gene, aip^X the *aip* gene originating from species *X* and $dpkA^Y$ indicates the *dpkA* gene originating from species *Y*.

2.4 Plasmid construction

In this section, the construction of plasmids used in this study is described. For simplicity, the description will be based on a plasmid containing a synthetic operon that comprises two genes.

The process of plasmid construction is composed of the following steps. First, plasmid DNA must be linearized through restriction digestion as preparation for gene insertion (Section 2.5.3). The next step is to amplify the genes for insertion into the plasmid by means of PCR. Primers must be designed such that the amplification product contains overlapping regions with the DNA ends to be joined. This step is performed with a proof-reading DNA polymerase, for example, CloneAmp polymerase, as described in Section 2.5.2. Next, Gibson assembly is used to combine the amplified DNA products and the linearized vector into a circular plasmid (Section 2.5.4). This mix is then transformed into cloning host *E. coli* DH5α, which is then cultivated overnight at 37 °C, and colony PCR is conducted to ensure the success of DNA assembly. Lastly, the clones considered positive in colony PCR are sequenced by Sanger sequencing to rule out any possible mutations. A schematic view of the entire process is shown in Figure 2.4.

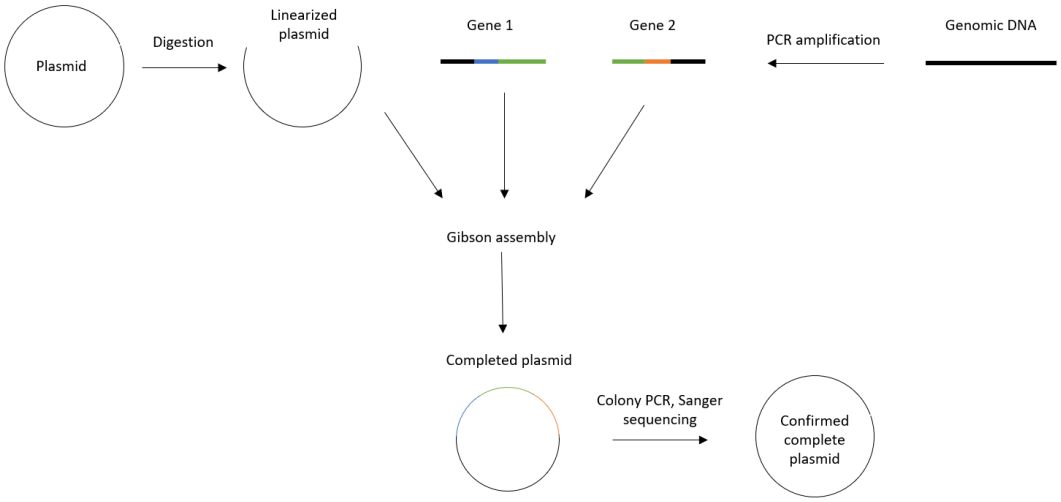

Figure 2.4: Illustration of the process utilized to construct plasmids in this study. The first step is linearizing the plasmid through enzyme digestion. Then the inserts to be inserted are amplified to include necessary overlapping regions. The amplified DNA sequences and the linearized plasmids are assembled into one plasmid through Gibson assembly. After that, the presence of inserts in the constructs is confirmed through colony PCR and Sanger sequencing.

2.5 Molecular cloning

2.5.1 Gel electrophoresis

It is often helpful to qualitatively verify the lengths of different DNA fragments through gel electrophoresis. In gel electrophoresis, DNA fragments are placed in separate wells within a gel, and a voltage is applied.

DNA strands exhibit evenly distributed negative charges along the DNA strand. Gel electrophoresis is based on this attribute. When a current is applied to DNA strands in the agarose gels, the DNA migrates toward the positive charge. Due to the pores contained in the gel, the DNA fragments are separated based on lengths, meaning that smaller fragments will travel further in the agarose gel than longer strands. Then the distance the DNA strands have traveled in the gel can be compared to a standardized DNA ladder.

To create the agarose, 0.8 % $\frac{w}{w}$ was added to Tris-Acetate-EDTA (TAE) buffer. The mix was then heated to dissolve the agarose in the solution. Then 20 µl of GelRed[45] was added per 400 mL of solution. 1 µl 6X DNA loading dye[46] was used for DNA loading. 6 µl of the 1 kb Plus DNA Ladder[47] was utilized in the study. Relevant recipes can be found in Section A.

2.5.2 Polymerase chain reaction

In order to amplify DNA fragments, polymerase chain reaction (PCR) can be utilized. The method is composed of 3 steps, denaturation, annealing, and elongation. In the first step, denaturation, the double-stranded DNA fragment is denatured into two single-stranded DNA fragments. The second step is annealing, in which primers added to the solution bind to the DNA fragments, creating a starting point for the DNA polymerase for the elongation process. It is crucial to determine the optimal annealing temperature of the primer, as primers are created for specific purposes and differ in G-C content, which leads to differences in annealing temperature between primers. Applying a too high annealing temperature will prevent the hybridization of the primers to the strand. At the same time, a too low annealing temperature will reduce the primer specificity, causing the primer to hybridize to unintended positions on the DNA strand. The annealing temperature was determined for the specific primer pairs with Clone Manager software.[48] The last step, elongation, occurs at the optimal temperature of

the DNA polymerase utilized for the specific PCR. In this step, the DNA polymerase extends the DNA along with the single-stranded DNA templates, creating the amplified product. The time required for this step depends on the DNA polymerase's elongation rate of the DNA polymerase and the amplified product length. For instance, GoTaq DNA Polymerase extends the DNA strand at a rate of 1kb/min, meaning that an amplified product of 10 kb would need an elongation time of 10 minutes. The PCR is set to repeat the steps described above in cycles, each cycle doubling the amount of the amplified product. After multiple cycles of three PCR steps, a final elongation step will ensure all the amplified DNA is double-stranded.

In this project two DNA polymerases were utilized, GoTaq[49] and Takara CloneAmp[50]. Because the CloneAmp polymerase is a high fidelity polymerase, it was utilized to amplify DNA that was then applied in molecular cloning. While the low-fidelity GoTaq polymerase was used for colony PCR (Section 2.10). The PCR mixes for each polymerase can be found in Table 2.4, 2.5. The PCR settings are shown in Table 2.6 and Table 2.7. To perform the PCRs the Mastercycler® Nexus X2 - PCR Thermal Cycler[51] was utilized.

Table 2.4: PCR reaction mix prepared for amplification using CloneAmp DNA polymerase.

Compound	Amount
CloneAmp Hifi PCR Premix	12.5 μl
Forward primer	0.5 μl
Reverse primer	0.5 μl
Genomic DNA	1.0 μl ($<$ 100 ng)
MilliQ water	10.5 μl

Table 2.5: PCR reaction mix prepared for amplification using GoTaq DNA polymerase.

Compound	Amount
Green buffer	2.00 μl
dNTPs	0.20 μl
Forward primer	0.20 μl
Reverse primer	0.20 μl
GoTaq polymerasee	0.05 μl
MilliQ water	7.35 μl

Table 2.6: PCR temperature cycling program used for Takara ClonAmp polymerase.

Step	Temperature [°C]	Time [sec]
Denaturation	98	10
Annealing	55	5-15
Elongation	72	5 kb^{-1}

Table 2.7: PCR temperature cycling program used for GoTaq polymerase.

Step	Temperature [°C]	Time [min]
Initial denaturation	95	10
Denaturation	95	0.5-1
Annealing	42-56	0.5-1
Elongation	72	1 kb^{-1}
Final extension	72	5

2.5.3 Digestion of plasmids

Plasmid DNA needs to be linearized in order to insert PCR-amplified DNA fragments containing targeted genes. To achieve this, restriction enzymes were used. The restriction enzyme recognizes specific sequences in DNA fragments and cleaves the DNA at these sites. The reaction mix utilized to digest plasmid DNA is shown in Table 2.8, while the restriction sites for the digestion with respective restriction enzymes employed in this study, PciI and BamHI, are shown in Figure 2.5.

Table 2.8: Reaction mix for digestion of plasmids.

Compound	Amount
Restriction enzyme	2 μl
3.1 (buffer)	10 μl
DNA	2 μg
MilliQ water	Complete to 100 μl

2.5.4 Gibson DNA-assembly

After obtaining linearized plasmid DNA and DNA fragments for insertion into the plasmid amplfied by PCR, Gibson assembly[52] was utilized to join ends of DNA fragments into a circular plasmid.

To successfully achieve DNA assembly, it is important to use the optimal ratio of plasmid DNA to insert DNA. The optimal relation was calculated using Equation 2.1. Ideally, 100 ng of the linearized plasmid DNA was used, which could then be used to calculate the amount of insert needed. The DNA parts were then mixed with the components displayed in Table 2.9 and placed in the Thermocycler for 1 hour at 50 °C. The assembly mix was then transferred to DH5α through heat-shock transformation. This process is described in Section 2.9.

$$Insert\ quantity\ (ng) = Vector\ quantity\ (bp)\ \cdot\ \frac{Insert\ size\ (bp)}{Vector\ size\ (bp)} \tag{2.1}$$

Table 2.9: Reaction mix for Gibson DNA assembly.

Compound	Amount
Gibson reaction mix	15 μl
Plasmid	100 ng
Insert	Calculated from Equation 2.1
MilliQ water	Complete mix to 20 μl

(a) BamHI restriction site.

(b) PciI restriction site.

Figure 2.5: Illustration of the BamHI (a) and the PciI (b) cutting sites in double stranded DNA.

2.6 DNA purification

The DNA materials used in this study, such as digested plasmid DNA and the PCR fragments, must be purified before they can be further utilized. This study utilized the QiAquick PCR Purification kit according to the manufacturer's protocol.[53]

2.7 Plasmid isolation

In this study, ZymoPURE Plasmid Miniprep was utilized to isolate plasmids.[54] To isolate plasmids with this kit, the first step was to grow 5 ml of bacterial culture harboring the wanted plasmid overnight. After this was done, the culture was spun down (13000 RPM, 5 min), and the protocol included in the kit is followed to complete the isolation.

2.8 Preparation of competent *E.coli* DH5α cell

In order to transform *E.coli* DH5α cells, the first step to be completed was to prepare competent *E. coli* DH5α cells. In this study, *E.coli* DH5α cells were first grown overnight. Then the cells were inoculated in a new subculture (300 ml) and grown until an OD_{600} of 0.3-0.4. After this, the cells were chilled on ice for 5 minutes, separated into six different Falcon tubes, and then centrifuged (4000 RPM, 4 °C) for 10 minutes. The supernatant was discarded, and the cells were resuspended in 15 ml chilled TfBI (Section A.8). After this, the cells were centrifuged (4000 RPM, 4 °C) for ten more minutes. The cells were then resuspended in 1 ml TfBII (Section A.9) and frozen at -80 °C.

2.9 Tranformation of *E. coli* by heat shock

To transform competent *E. coli* DH5α cells, the first step was to add the desired plasmid DNA to 100 µl competent cells and incubate the mixture on ice for 20 minutes. After that, the DNA-cell mix was heat shocked in a water bath at 42°C for 45 seconds. The cells were then left on ice for 90 seconds. Then, 1 ml of lb medium was added, and the cells were kept in a shaking incubator (200 rpm) at 37 °C for 45-60 minutes. Then, the cells were spun down, and the supernatant was discarded. The pellet was then plated on an LB plate with suitable antibiotics and left overnight for inoculation at 37 °C.

2.10 Colony PCR

After the product of Gibson assembly reaction had been transformed into *E. coli*, confirmation of the correctness of constructs is necessary. The presence of the insert in these plasmids was checked through colony PCR. To perform colony PCR, 15 colonies of the transformed *E. coli* cells containing the product from the Gibson assembly were restreaked onto a new master plate with pipette tips and inoculated overnight. At the same time, the tips with remaining *E. coli* cells were added to separate PCR tubes containing the mix described in Table 2.5. PCR reaction was then conducted according to the protocol in Table 2.7, and the product length amplification was checked with gel electrophoresis.

2.11 Preparation of plasmids for Sanger sequencing

After colony PCR has confirmed the correctness of the length of the constructed plasmids, it is crucial to confirm that the plasmids do not contain mutations that do not alter the length of the plasmid. This can be achieved by Sanger sequencing. In order to sequence the constructed plasmid, the first thing to be done is to mix 2.5 ml of the isolated plasmid ($\sim$ 70 ng/µl) with 7.5 ml of primer ($\sim$ 100 µM). It is essential to select primers that amplify the regions cotaining the new inserts in the plasmid. The mixes were then sent to Eurofins for sequencing. After the sequencing was complete, the sequences was aligned with the theoretical plasmid utilizing the Clone Manager software.

2.12 Preparation of electrocompetent *B. methanolicus* cells

In order to transform *B. methanolicus* the first step to be completed was to prepare electrocompetent *B. methanolicus cells*. In this study, *B. methanolicus* cells were first grown overnight. Then the cells were inoculated in a new subculture at an OD_{600} of 0.1 - 0.2. After four hours, the culture was reinoculated to an OD_{600} of 0.05 and grown until the OD_{600} was 0.25. Once an OD_{600} of 0.25 was reached, 50 ml of the cultures were spun down (7,800 RPM, 40 °C), the supernatant was poured off, and the cells were resuspended in 4.5 mL electroporation buffer (EPB). Then, the cells were centrifuged for 10 minutes, and the supernatant was removed. The same process was then repeated with 9 mL EPB. After that, the supernatant was poured off, and the cells were resuspended in the remaining liquid. 100 µl of the mix was then aliquoted into separate sterile Eppendorf tubes and stored at - 80 °C.

2.13 Transformation of electrocompetent *B. methanolicus*

In this study, first electrocompetent cells and the plasmid DNA were mixed in Eppendorf tube, transferred to a cold electroporation cuvette, and left on ice for 30 minutes. Then, after the 30 minutes, the mixes were electroporated at 200 Ω, time constant 4.5-5.5 and 12.5 kV/cm. Immediately after that, 1 ml of the prewarmed SOB medium was added. Then the mix was transferred into a flask containing 12.5 ml previously prewarmed SOB medium. The cells were then incubated (50 °C, 200 rpm) for 6 hours. After the 6 hours, the cultures were spun down, resuspended in 100 µl SOB medium, and plated on an SOB plate supplemented with suitable antibiotics. After that, the plates were incubated at 50 °C overnight. The following day, three colonies were picked and incubated in MVcMY medium supplemented with suitable antibiotics overnight. The day after, the cultures were inoculated into subcultures of the same medium and grew until the OD_{600} reached 2.0 - 2.5. At this point, the cultures were utilized to prepare glycerol stocks and frozen at -80 °C.

2.14 Preparation of glycerol stocks

In order to prepare glycerol stocks for storing *B. methanolicus* strains at -80 °C, the *B. methanolicus* colonies were inoculated into MVcMY medium supplemented with suitable antibiotics and grown until an OD_{600} of 2.0 - 2.5. Then, 1.5 mL of bacterial culture was mixed with 4.5 ml of glycerol solution (Section A.7) and then placed in the freezer at -80 °C. For *E. coli*, the colony was inoculated in LB medium supplemented with suitable antibiotics and cultivated overnight. The glycerol stock was prepared by mixing 3.5 ml bacterial culture with 6.5 ml glycerol solution.

2.15 Amino acid quantification with high-performance liquid chromatography

High-performance liquid chromatography (HPLC) is a technique used to quantify the concentrations of different compounds in a mixture. In HPLC, the sample is added to a solvent, which is passed through a column under high pressure. The solvent is called the mobile phase, while the column is called the stationary phase. The stationary phase typically contains a material that separates the solute based on a given criterion, in this case, polarity. As the mobile phase is passed through the column, the different components will elute separately, and when these are compared with pure standards, it is possible to estimate the amount of compound contained in the sample.

In this study, the FMOC-CL (fluorenylmethyloxycarbonyl chloride) method was utilized to derivatize amino acids in order to enable their detection. [55] This protocol attaches a fluorescent molecule to amino acids contained in the sample investigated, which was then detected by the 2475 FLR Detector [56] as the sample left the HPLC. As different amino acids exhibit different polarities, the column will retain them for different lengths of time, and they will therefore elute at different times. This leads the detector to measure fluorescent peaks at different

times, making it possible to separate the different compounds. It was then possible to compare these peaks with standards of amino acids of known concentrations in order to quantify the concentrations of amino acids contained in the samples in question. The Waters e2695 was the instrument utilized.[57] The column utilized was Symmetry C18 by Waters (100 Å, 3.5 m, 4.6 mm × 75 mm).[58] The flow rate and composition of the mobile phase is shown in Table 2.10. The concentrations of the standards were 0, 6.25 mM, 12.5 mM, 25 mM, 50 mM, and 100 mM of the compound investigated.

Table 2.10: Flow rate and composition of mobile phase during the HPLC run. A - 50 mM Na-acetate, pH 4.2, B - organic solvent acetonitrile. Table adapted from[12].

Program time [min]	Flow rate [ml min^{-1}]	% A	% B
0	1.3	62.0	38.0
5	1.3	62.0	38.0
12	1.3	43.0	57.0
14	1.3	24.0	76.0
15	1.3	43.0	57.0
18	1.3	62.0	38.0

3 Results

3.1 Construction of plasmids towards heterologous gene expression in *B. methanolicus*

The plasmids created in the study are listed below.

1. pBV2xp-aip^{SjBi}-$dpkA^{Ps}$
2. pBV2xp-aip^{SjBi}-$dpkA^{Pp}$
3. pBV2xp-aip^{Tv}-$dpkA^{Ps}$
4. pUB110Smp-*katA*

3.1.1 Digestion of the pBV2xp plasmid

The pBV2xp plasmid was linearized by the restriction enzyme BamHI, as shown in Figure 3.1 where one band of DNA is visible. The expected length of the fragment was 8,104 bp (the legnth of the pBV2xp plasmid), which is consistent with the band shown in Figure 3.1. If the digestion had been incomplete, multiple bands would be visible, which is characteristic of circular DNA.

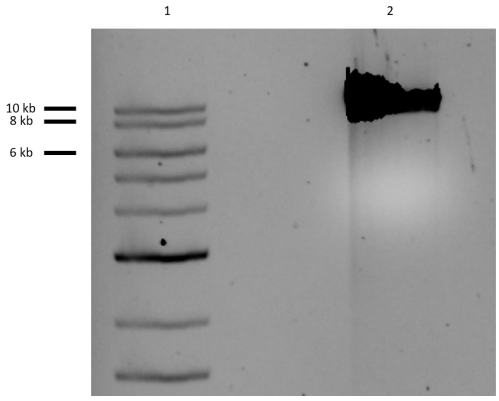

Figure 3.1: Gel picture of the 0.8 % agarose gel electrophoresis of the digested pBV2xp plasmid. Well 1 shows the DNA ladder. Well 2 shows pBV2xp digested by BamHI-HF.

Figure 3.1 shows a single band overlapping the length of 8,104 bp, indicating that the digestion was successful.

3.1.2 Amplification of genes

The inserts for pBV2xp were PCR-amplified, as described in Section 2.5.2. The amplification was checked by gel electrophoresis, shown in Figure 3.2.

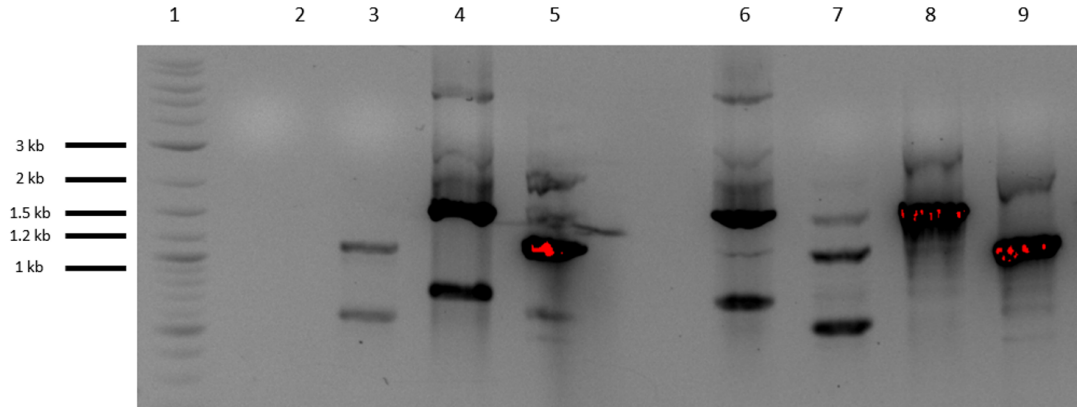

Figure 3.2: Gel picture of the 0.8 % agarose gel electrophoresis of the PCR amplified genes, aip^{Tv}, aip^{SjBi}, $dpkA^{Ps}$ and $dpkA^{Pp}$ for insertion in pBV2xp. Well 1 shows the DNA ladder. Wells 8 and 9 are related to another project. Wells 2 shows the amplification of aip^{Tv} expected to be 1,941 bps long, while well 3 shows the corresponding amplification of $dpkA^{Ps}$ expected to be 1,119 bps long. Wells 4 and 6 show the different amplifications of the aip^{SjBi} genes expected to be 1575 bp long, while 5 and 7 show the amplification of $dpkA^{Ps}$ and $dpka^{Pp}$, expected to be 1126 and 1090 bps long, respectively.

The expected DNA fragment lengths of the amplification are displayed in Table 3.1, along with the corresponding wells in which these were placed.

Table 3.1: Expected lengths of amplifications of various genes simulated in the Clone Manager software.

Plasmid	Gene	Expected lengths [bp]	Well in Figure 3.2
pBV2xp-aip^{Tv}-$dpkA^{Ps}$	aip^{Tv}	1,941	2
pBV2xp-aip^{Tv}-$dpkA^{Ps}$	$dpkA^{Ps}$	1,119	3
pBV2xp-aip^{SjBi}-$dpkA^{Ps}$	aip^{SjBi}	1,575	4
pBV2xp-aip^{SjBi}-$dpkA^{Ps}$	$dpkA^{Ps}$	1,126	5
pBV2xp-aip^{SjBi}-$dpkA^{Pp}$	aip^{SjBi}	1,575	6
pBV2xp-aip^{SjBi}-$dpkA^{Pp}$	$dpkA^{Pp}$	1,090	7

From Figure 3.2 and Table 3.1 it is clear that all the genes were amplified successfully, except for aip^{Tv}. This is seen as the bands of the amplified genes overlap with the simulated lengths expected to be present, while the amplification of aip^{Tv} shows no band, meaning that no amplification occurred. Multiple attempts were conducted to amplify aip^{Tv}, and these attempts were unsuccessful.

3.1.3 Confirmation of constructs through colony PCR

The PCR products from Section 3.1.2 and the linearized plasmids from Section 3.1.1 were joined through Gibson assembly and transformed into *E. coli*. Colony PCR was performed in order to confirm a successful assembly. The colony PCR products from *E. coli* transformed with Gibson assembly mix for plasmid pBV2xp-aip^{SjBi}-$dpkA^{Ps}$ are shown in Figure 3.3, while pBV2xp-aip^{SjBi}-$dpkA^{Pp}$ are shown in Figure 3.4.

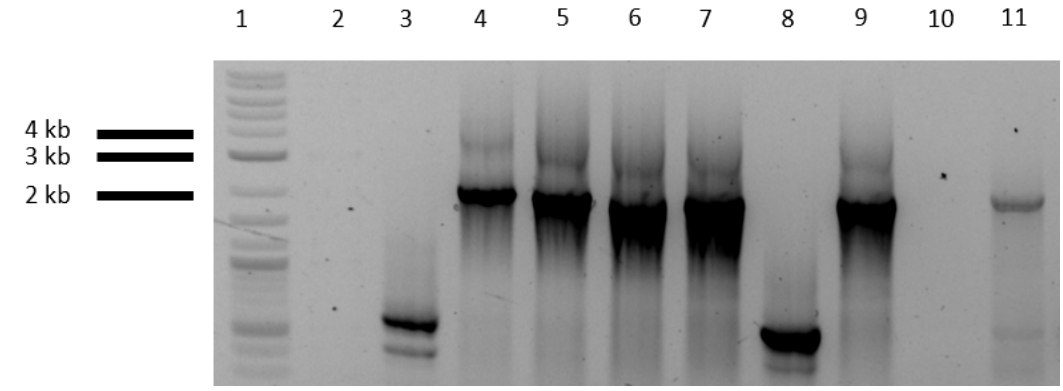

Figure 3.3: Gel electrophoresis with 0.8 % agarose gel picture.. Well 1 is the DNA ladder. Well 1: the DNA ladder. Wells 2-11: colony PCR products of *E. coli* cells transformed with Gibson assembly product. Size of the band for positive clone: 3,155 bps.

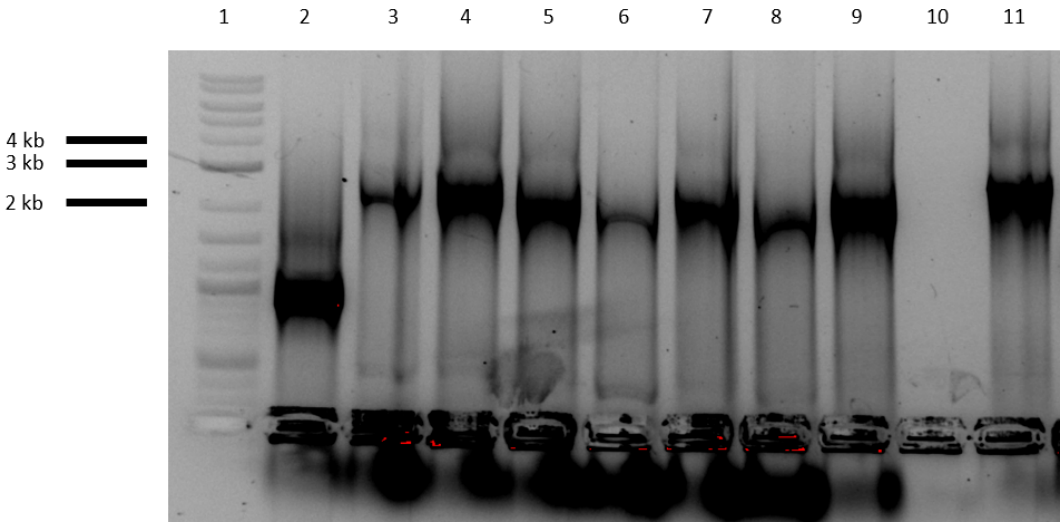

Figure 3.4: Gel electrophoresis with 0.8 % agarose gel picture. Well 1: the DNA ladder. Wells 2-11: colony PCR products of *E. coli* cells transformed with Gibson assembly product. Size of the band for positive clone: 3,122 bps.

In Figure 3.3 a positive clones are present in wells 4-7, 9, 11, while 3.4 exhibits positive hits in well 3-9 and 11. Some clones were sent to Sanger sequencing, and exhibited no problematic mutations. The alignment can be seen in Section C

3.1.4 Construction of pUB110Smp-*katA*

In this study an attempt was made to construct pUB110Smp-*katA*. As described Section B, pUB110Smp could not be digested, making the construction of the plasmid unsuccessful.

3.2 Methanol-based production of 5AVA

This study attempted to produce 5AVA in the recombinant *B. methanolicus* strains heterologously expressing the *aip* gene from various genetic donors and overexpressing *katA* gene (Table 2.2). The strains were cultivated in MVcM with supplementation of 0.001 % ($\frac{v}{v}$) hydrogen peroxide, and the growth was monitored for 10 hours through measurement of OD_{600}

every 2 hours. An HPLC sample was then taken after 26 hours of growth. The growth of the bacterial cultures is shown in Figure 3.5.

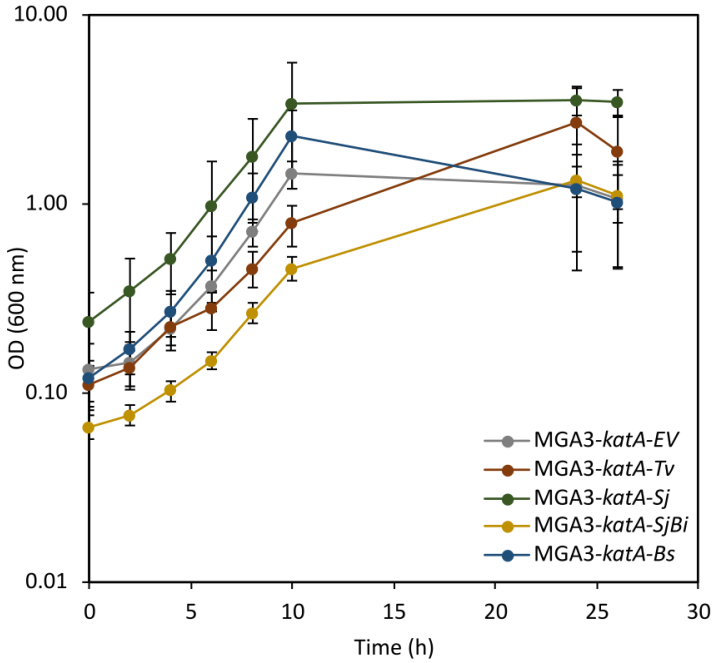

Figure 3.5: Growth of recombinant *B. methanolicus* strains heterologously expressing the *aip* gene from various genetic donors and overexpressing *katA* gene in MVcM supplemented with 0.001 % ($\frac{v}{v}$) hydrogen peroxide. Error bars are standard deviations, and the data points displayed are the mean OD_{600} of technical triplicates.

All strains grew exponentially in the first 10-hour growth phase, except for the MGA3-*katA-Tv* strain, which exhibited an unexpected decrease in growth after 4 hours. The growth rates and the concentration of 5AVA were determined as displayed in Table 3.2. The MGA3-*katA-Sj* and MGA3-*katA-Tv* strains exhibited the highest production of 5AVA.

Table 3.2: Calculated 5AVA concentrations and growth rates of recombinant *B. methanolicus* strains cultivated in MVcM medium supplemented with 0.001 % ($\frac{v}{v}$) hydrogen peroxide. Errors are standard deviations.

Strain	Growth rate [h^{-1}]	5AVA [mg/l]
MGA3-*katA-EV*	0.32 ± 0.01	0.00 ± 0.00
MGA3-*katA-Bs*	0.35 ± 0.04	0.00 ± 0.00
MGA3-*katA-SjBi*	0.25 ± 0.01	1.19 ± 1.60
MGA3-*katA-Sj*	0.32 ± 0.02	21.41 ± 11.72
MGA3-*katA-Tv*	0.24 ± 0.01	8.83 ± 6.63

3.3 Determination of 5AVA concentration throughout the bacterial growth phase in *B. methanolicus*

In the cultivation of 5AVA producing strains, the strain MGA3-*katA-Tv* presented a deviation in its growth. Figure 3.5 shows growth impairment in this strain between 4-6 hours. This might indicate that the strain is affected by the accumulation 5AVA, as this compound previously has been shown to be toxic to *B. methanolicus*.[27] Therefore, it was decided to monitor 5AVA concentration throughout the growth of the recombinant *B. methanolicus* strains harboring the *katA* and *aip* genes to determine whether the strains remove 5AVA to cope with its toxicity.

A growth experiment was performed in similar conditions to the one described in Section 3.2. However, an HPLC sample was taken every four hours throughout the bacterial growth. The growth curves of tested strains are shown in Figure 3.6.

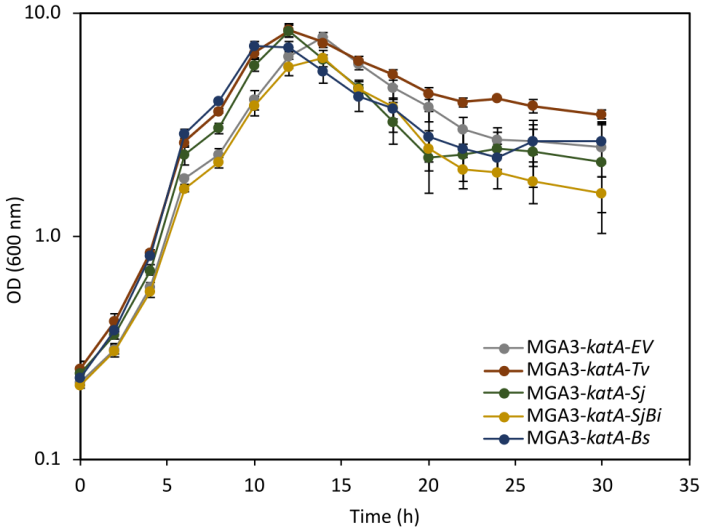

Figure 3.6: Growth of recombinant B. methanolicus strains heterologously expressing the *aip* gene from various genetic donors and overexpressing *katA* gene in MVcM supplemented with 0.001 % ($\frac{v}{v}$) hydrogen peroxide. Error bars are standard deviations, and the data points displayed are the mean OD_{600} of technical triplicates.

The *B. methanolicus* strain grew exponentially in the first 6 hours of the cultivation. The growth rates were determined and displayed in Table 3.3.

Table 3.3: Calculated growth rates of recombinant MGA3 strains cultivated in MVcM medium supplemented with 0.001 % ($\frac{v}{v}$) hydrogen peroxide. Errors are standard deviations.

Strain	Growth rate [h^{-1}]
MGA3-*katA-EV*	0.35 ± 0.01
MGA3-*katA-Bs*	0.42 ± 0.01
MGA3-*katA-SjBi*	0.33 ± 0.01
MGA3-*katA-Sj*	0.38 ± 0.01
MGA3-*katA-Tv*	0.39 ± 0.02

The concentrations of 5AVA and L-lysine over time were determined as shown in Figure 3.7. The L-lysine concentrations show a clear upward trend in all strains, while the 5AVA concentrations seem to increase until about 20 hours in the experiment and then stabilize.

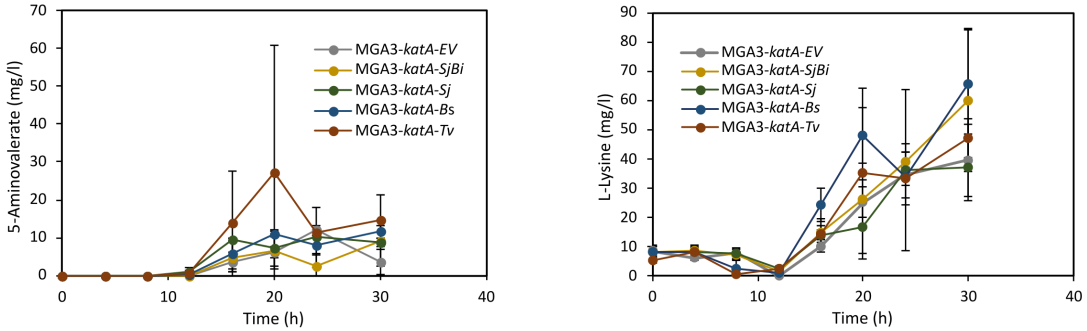

(a) 5AVA concentrations over time.

(b) L-Lysine concentrations over time.

Figure 3.7: 5AVA (a) and L-lysine (b) production of various recombinant *B. methanolicus* strains cultivated in MVcM medium supplemented with 0.001 % ($\frac{v}{v}$) hydrogen peroxide over time. Errors are standard deviations of technical triplicates.

3.4 The feasibility of *B. methanolicus* as a potential host for LPA production

3.4.1 Pipecolic acid toxicity

Before analyzing the created strains regarding LPA production, it was of interest to test the LPA toxicity in *B. methanolicus*. A growth experiment with wild type *B. methanolicus* MGA3 was performed, where 0 mM, 6.25 mM, 12.5 mM, 25 mM, 50 mM, or 100 mM of LPA was supplemented to MVcM medium to determine if the growth rate would be affected by LPA supplementation. The growth of MGA3 with various supplementations of LPA is shown in Figure 3.8.

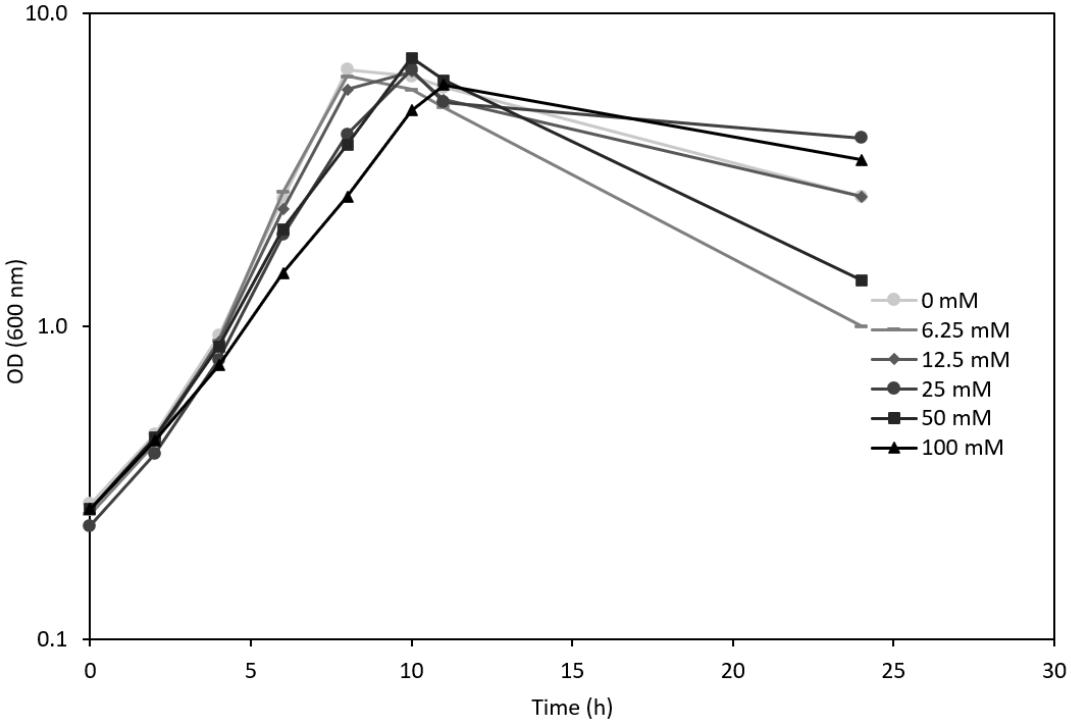

Figure 3.8: Growth of *B. methaolicus* MGA3 in MVcM medium supplemented with increasing concentrations of LPA. MGA3 was exposed to 0 mM, 6.25 mM, 12.5 mM, 25 mM, 50 mM and 100 mM LPA.

This experiment was conducted with only one replicate, meaning it is impossible to estimate a standard deviation. As seen in Figure 3.8, the cultures with a higher concentration of supplemented LPA tend to grow slower. The growth rates were then calculated and plotted against LPA concentration to create Figure 3.9.

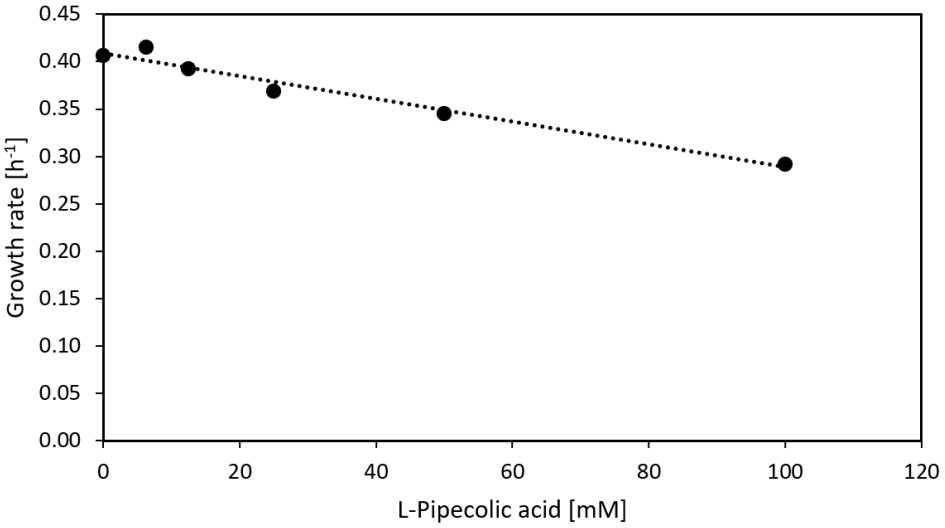

Figure 3.9: Growth of rates of MGA3 in MVcM medium supplemented with 0 mM, 6.25 mM, 12.5 mM, 25 mM, 50 mM or 100 mM LPA. The dotted line represents a data trendline, which gives the linear relation between growth rate and LPA concentration, with an R^2 of 0.9689.

Lethal concentration 50 (LC_{50}) represents the concentration at which the growth rate of a bacterial culture is reduced by 50 %. In this case, where the growth rate of *B. methanolicus* with no supplementation of LPA was 0.41 h^{-1}, the LC_{50} would be reached when the growth rate is 0.21 h^{-1}. In Figure 3.9 this is represented by the halfway point between the x-axis and the leftmost data point. Assuming the linear relation calculated between LPA concentration and growth rate of *B. methanolicus*, the growth rate of 0.21 h^{-1} is reached when the concentration of LPA is 170 mM, meaning that the LC_{50} of LPA for *B. methanolicus* can be estimated to be 170 mM.

3.4.2 LPA as carbon or nitrogen source for *B. methanolicus*

To determine whether *B. methanolicus* can utilize LPA as either a carbon or nitrogen source, the nitrogen and carbon sources in the MVcM medium were replaced with LPA in two separate experiments, one where the nitrogen source (ammonium sulfate) was replaced and one where the carbon source (methanol) was replaced. The concentration of LPA used to replace was determined such that the number of nitrogen or carbon atoms stayed the same in the medium. This works out to be a concentration of 33 mM LPA as carbon source and 32 mM LPA when used as nitrogen source. Standard MVcM media was used as control. The growth was observed by means of OD_{600} and is shown in Figure 3.10.

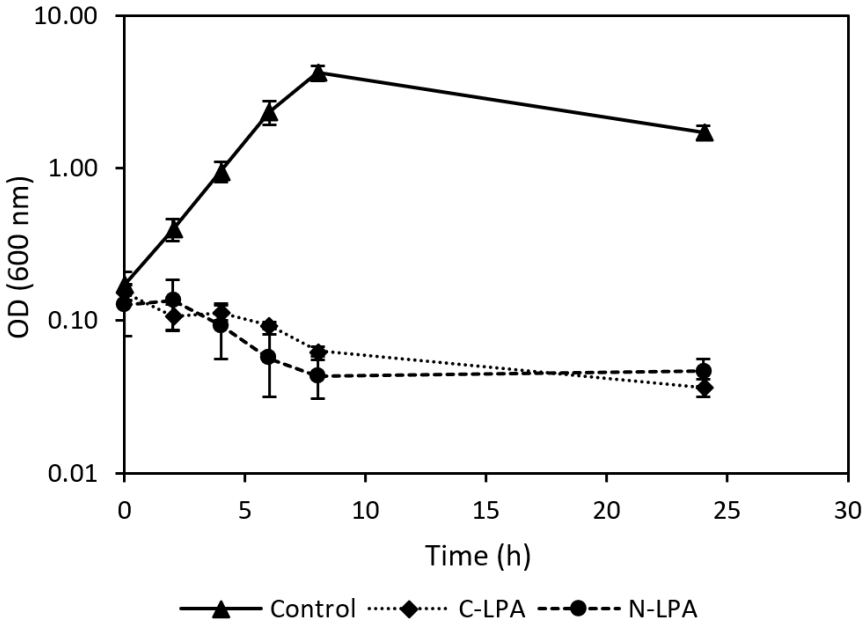

Figure 3.10: Growth of MGA3 in MVcM where the carbon source has been replaced with LPA (C-LPA), the nitrogen source has been replaced with LPA (N-LPA), and control with standard MvCM media (Control). Error bars are standard deviation, and the datapoint displayed is the mean OD_{600} of technical triplicates.

The growth curves in Figure 3.10, show that *B. methanolicus* cannot utilize LPA as either carbon or nitrogen source as the sole nitrogen or carbon source to sustain growth as there is no increase in OD_{600} for these cases.

3.5 Methanol-based production of LPA

To determine the production of LPA in the recombinant *B. methanolicus* strains overexpressing a *katA* gene and heterologously expressing a combination of *aip* and *dpkA* genes from different genetic donors were cultivated in MVcM, and the growth was measured. Then a sample of supernatant was taken after 26 hours of growth for analysis by HPLC. The growth of the recombinant *B. methanolicus* strains is shown in Figure 3.11.

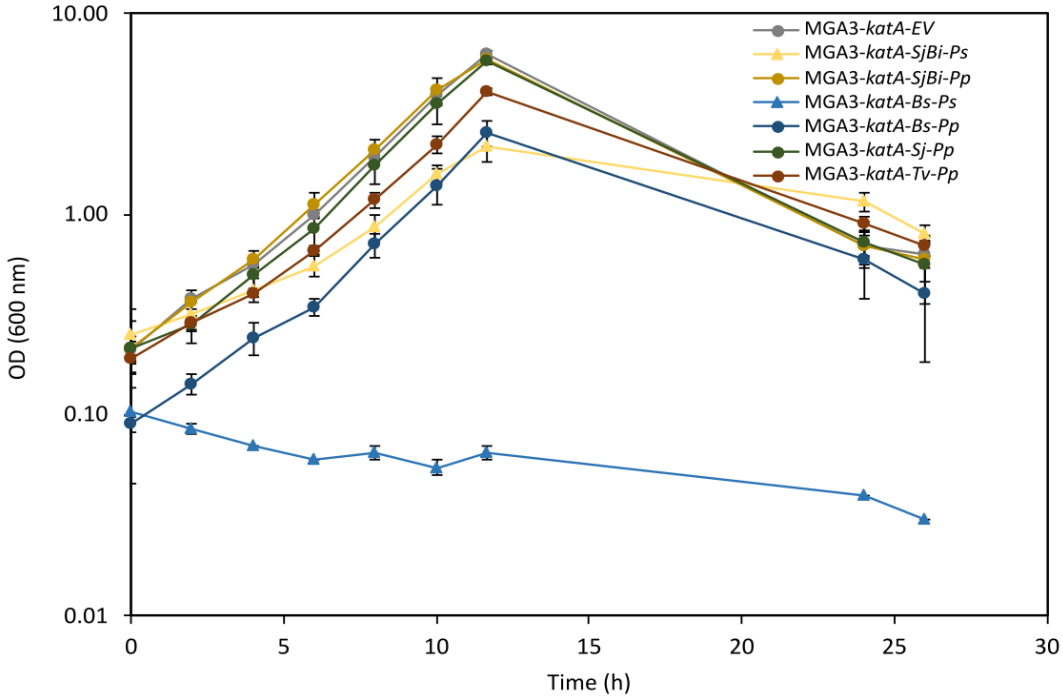

Figure 3.11: Growth in MVcM of recombinant *B. methanolicus* strains overexpressing a *katA* gene and heterologously expressing a combination of *aip* and *dpkA* genes from different genetic donors. Error bars are standard deviation, and the data point displayed is the mean OD_{600} of technical triplicates.

As seen from Figure 3.11 all of the strains grew exponentially during the first 12 hours, except for MGA3-*katA-Bs-Ps*, which did not grow at all. The growth rates and LPA concentrations were then determined using HPLC and are displayed in Table 3.4.

Table 3.4: LPA concentrations determined by HPLC and growth rates of recombinant *B. methanolicus* strains cultivated in MVcM medium.

Strain	Growth rate [h^{-1}]	LPA [mg/l]
MGA3-*katA-EV*	0.34 ± 0.02	0.92 ± 0.03
MGA3-*katA-Bs-Ps*	0.00 ± 0.00	-
MGA3-*katA-Bs-Pp*	0.35 ± 0.03	17.14 ± 7.51
MGA3-*katA-SjBi-Ps*	0.25 ± 0.02	3.07 ± 0.40
MGA3-*katA-SjBi-Pp*	0.31 ± 0.01	3.83 ± 0.47
MGA3-*katA-Sj-Pp*	0.35 ± 0.02	15.42 ± 1.73
MGA3-*katA-Tv-Pp*	0.31 ± 0.01	15.83 ± 4.75

As depicted in Table 3.4, MGA3-*katA-Bs-Pp*, MGA3-*katA-Sj-Pp* and MGA3-*katA-Tv-Pp* produced more LPA compared to the other strains.

3.6 Effect of induction time on LPA production

The first attempt at producing LPA utilizing the recombinant *B. methanolicus* strains discussed in this study resulted in no production of the compound. This led to the experiment described in Section 3.5, where the expression of *aip* and *dpkA* genes was induced after 6 hours instead at T=0, and LPA production was achieved. Based on the resulting data, a new experiment was designed to optimize induction times for LPA production. The experiment was carried out for one of the best-performing strains of the previous experiment, MGA3-*katA-Sj-Pp*. In

this experiment, the expression of *aip* and *dpkA* was induced at different times to optimize the induction time. The growth of the MGA3-*katA*-*Sj*-*Pp* in different conditions is shown in Figure 3.12.

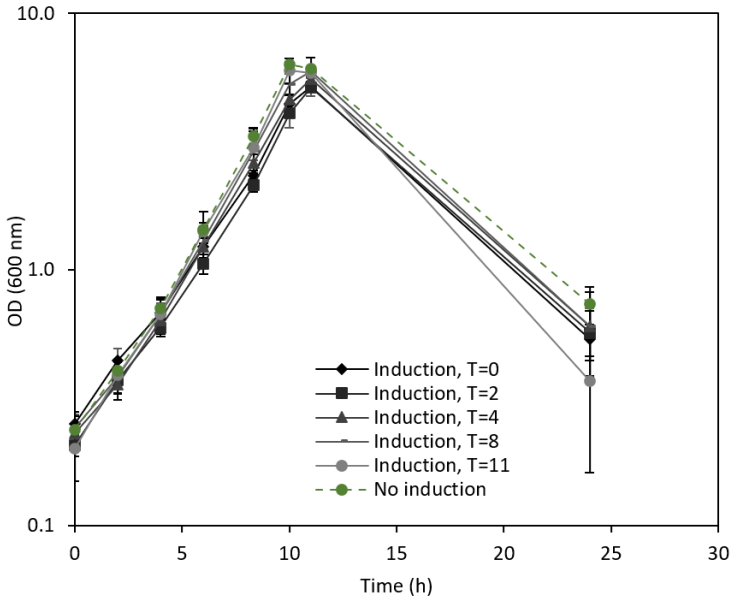

Figure 3.12: Growth of MGA3-*katA*-*Sj*-*Pp* induced with 1 % $\frac{w}{v}$ xylose after 0 h, 2 h, 4 h, 8 h, or 11 h after inoculation. Error bars are standard deviations, and the data points displayed are the mean OD_{600} of technical triplicates.

The production of LPA, L-lysine, and 5AVA was determined using the HPLC, and the growth rates were calculated using the growth data. The results are displayed in Table 3.5 and show that the highest LPA concentrations were achieved when inducing after 4 hours. The growth rates increased with the delay of the induction time, indicating the metabolic burden of heterologous gene expression on the cell growth.

Table 3.5: Calculated LPA, L-lysine, 5AVA concentrations, and growth rates of MGA3-*katA*-*Sj*-*Pp* cultivated in MVcM medium when induced at different times. Errors are standard deviations.

Inoculation time [h]	Growth rate [h^{-1}]	LPA [mg/l]	L-Lysine [mg/l]	5AVA [mg/l]
0	0.28 ± 0.01	6.53 ± 4.40	217.21 ± 119.03	4.68 ± 6.61
2	0.29 ± 0.01	14.63 ± 1.14	137.75 ± 47.65	8.05 ± 4.89
4	0.31 ± 0.01	18.13 ± 12.04	150.85 ± 12.84	15.39 ± 16.51
8	0.31 ± 0.00	14.47 ± 12.04	128.20 ± 29.81	9.47 ± 1.57
11	0.34 ± 0.00	13.75 ± 3.47	123.81 ± 9.03	77.22 ± 69.49
No induction	0.35 ± 0.031	4.35 ± 0.00	104.17 ± 33.95	6.44 ± 1.93

4 Discussion

4.1 Methanol-based 5AVA production

Previously, it has been reported that 5AVA does not support growth of *B. methanolicus* as sole nitrogen or sole carbon source.[27] It is unclear if the organism lacks a system to import 5AVA into the cell or if there is a lack of genes for catabolism of 5AVA in its genome. 5AVA, however, is toxic to *B. methanolicus*, suggesting that it could be the latter. The inhibition of *B. methanolicus* by 5AVA likely causes the titers found in this study to be lower than they otherwise would be, as the compound represses the growth of *B. methanolicus* and, likely, 5AVA production.

The supplementation of hydrogen peroxide to the bacterial cultures with the aim to increase 5AVA production increased production by strains overexpressing aip^{Sj} and aip^{SjBi} strains, compared to no production without hydrogen peroxide supplementation and *katA* overexpression tested previously.[12] This indicates that the presence of hydrogen peroxide helps the spontaneous conversion of α-ketolysine into 5AVA. Overexpressing aip^{Tv} in *B. methanolicus* was previously found to produce the most 5AVA, with no supplementation of hydrogen peroxide and overexpression of *katA*. In the present study, however, when aip^{Tv} was overexpressed in conjuction with *katA* and supplemented with hydrogen peroxide, the titer of 5AVA decreased from 20 mg/l to 8.83 mg/l, as compared to when not overexpressing *katA*. It is possible that this strain produced 5AVA until its growth was impaired, leading to the degradation of 5AVA through the activation of some unknown metabolic response. As seen in Figure 3.5, after four hours of growth for MGA3-*katA-Tv*, the growth was stunted unexpectedly, which might indicate that this is taking place.

Previously, a 5AVA tolerant strain was created through adaptive laboratory evolution (ALE), however, the genetic background directly responsible for the increased 5AVA resistance was not identified.[27] The ALE-created strain can possibly be used in 5AVA production as an alternative to *B. methanolicus* MGA3, which was utilized in this study. If pTH1mp-*katA* is transformed into this strain along with the overexpression of the *aip* gene, a greater titer of 5AVA might be achieved because 5AVA will not have a similar inhibitory effect on growth.

When monitoring the 5AVA concentrations throughout the growth of the recombinant *B. methanolicus* strains overexpressing *aip* genes, the goal was to uncover the pattern of 5AVA accumulation during growth and investigate the possibility of 5AVA degradation. As shown in Figure 3.7, it appears that the titers of 5AVA are at their maximum at around 20 hours and that they decrease after that, indicating that 5AVA degradation might take place in *B. methanolicus*. However, the uncertainties associated with these values are so significant that it is difficult to make any definite deduction based on this data. The control strain MGA3-*katA-EV* also produces a lot of 5AVA in this experiment, raising questions as to how reliable the data collected really is.

The L-lysine α-oxidases have different temperature optimums from the cultivation conditions utilized for *B. methanolicus* in this study. Aip^{Sj}, for example, has an optimal temperature of 70 °C.[35] To improve the metabolic flux through the first step of the pathway, a gene with a closer optimal temperature should be considered, given that one exists.

To the authors' knowledge, this is the first report of 5AVA production from methanol with supplementation of hydrogen peroxide supporting the spontaneous conversion of α-ketolysine to 5AVA in *B. methanolicus*. Supplementation of hydrogen peroxide has not been attempted before in *B. methanolicus*, due to the high susceptibility of the species to the compound. Therefore, the overexpression of catalase was likely instrumental in achieving higher titers of 5AVA as it decreased the organism's susceptibility toward hydrogen peroxide in some of the strains. The supplementation, however, did not increase the maximum achieved titer as compared to the previous overexpression of *aip* genes in *B. methanolicus*.[12] It is also worth mentioning that the hydrogen peroxide concentration of 0.001 % (v/v) used in this study is

below a threshold of inhibitory effect previously shown for *B. methanolicus* MGA3 at 0.005 %,[41] and could possibly be increased to 0.002-0.004 %, though a susceptibility study has to be performed to confirm this.

4.2 Methanol-based LPA production

LPA was found to impair the growth of *B. methanolicus*. LPA has previously been shown to be devoid of inhibitory activity in *E. coli*[59], suggesting an organism-specific impairment. However, the study only tested a concentration of 0.77 mM LPA, orders of magnitude less than what was tested on *B. methanolicus* in this study. The LC_{50} was estimated to be 170 mM. This value, however, assumed a linear relationship between the concentration of LPA and the growth rate of *B. methanolicus*. The assumption that the relationship between the two is linear is not necessarily true. The inhibitory relation can often take the form of another curve, e.g., an S-curve.[60] Since there is a noticeable reduction in growth at higher concentrations of LPA, developing an LPA-resistant strain might be considered for improved LPA production. However, the LC_{50} found in this study is about a thousand times the production of LPA reached, meaning other measures probably are better for immediate improvement of LPA production in *B. methanolicus*. As seen in Figure 3.10, *B. methanolicus* cannot utilize LPA as a sole carbon or nitrogen source, eliminating some concerns of degradation of the compound.

The strains producing the highest titers og LPA in this study was MGA3-*katA-Bs-Pp*, MGA3-*katA-Sj-Pp*, and MGA3-*katA-Tv-Pp*, producing 17.14 ± 7.51, 15.42 ± 1.73 and 15.83 ± 4.75, respectivly. These include two of the best performing *aip* genes from the recombinant 5AVA-producing *B. methanolicus* strains, which is in line with expectations, as when more α-ketolysine is produced, more LPA should also be produced.

Previously, when *B. methanolicus* overexpressed the *aip* and *dpkA* genes no production of LPA was reached.[40] In this study, when also overexpressing catalase, LPA production was achieved. This is in line with expectations, as when α-ketolysine is in the presence of hydrogen peroxide, it is expected to form 5AVA (Figure 1.5). Therefore, the removal of hydrogen peroxide was likely necessary for the increased production of LPA determined in this study.

In this study, the production of LPA by *B. methanolicus* was observed when no *aip* or *dpkA* genes were overexpressed, however, while overexpressing *katA*. The titer achieved was not very high at 0.92 ± 0.03 mg/l. It can be speculated that a native enzyme of *B. methanolicus* exhibits L-lysine α-oxidase activity and produces α-ketolysine, which is then converted to LPA in the absence of hydrogen peroxide caused by catalase activity. Importantly, in such a case, a native enzyme of *B. methanolicus* would have to exhibit DpkA (Δ^1-piperideine-2-carboxylate reductase) activity. The other possibility is that the overexpression of catalase hinders some other reaction that utilizes hydrogen peroxide in *B. methanolicus*, creating another unknown metabolite with similar elution time in the HPLC as LPA. This hypothesis is substantiated by what appears as two peaks overlapping on the chromatogram from the HPLC, where the LPA peak is supposed to be located. This peak was also observed on the other recombinant strains overexpressing *aip* or *dpkA*. This would make sense, as the catalase should also redirect the same metabolic pathway in these strains by removing hydrogen peroxide.

The induction time best suited for overexpressing recombinant genes in *B. methanolicus* was after 4 hours as seen in Table 3.5. This is in contrast with the expectation that the best results would be achieved if induced from the beginning, as this would allow the production of LPA during the entire growth phase of the bacterial culture, providing more time to produce the compound but slowing down the growth rate. However, this substantiates the effectiveness of the traditionally utilized induction time of 2 hours. This time, however, did not achieve better results than induction after 4 or 8 hours, as stated earlier. This experiment achieved production of LPA (4.35 ± 0.00 mg/l) for the bacterial culture that was not induced, meaning that the data from this experiment is highly dubious and the experiment should be duplicated to acquire more reliable data.

Interestingly, during the experiment optimizing the induction time, the bacterial strains produced 5AVA. This indicates that the catalase activity in the recombinant strains is insufficient, allowing part of the metabolic flux to enter the competing pathway. This sets a clear target for improving the production of LPA, increasing the exhibited catalase activity of the strains. This can be achieved by either integrating a second copy of catalase into the genome of *B. methanolicus*, or increasing the expression of the gene either through the use of a high copy number plasmid or a more potent promoter. This study attempted to increase the expression of the endogenous catalase by use of a high copy number plasmid pUB11Smp for *katA* expression in *B. methanolicus*. However, the construction of this plasmid failed, as discussed in Section B.

Additionally, an attempt to overexpress the L-lysine cyclodeamination pathway should be made, as this pathway previously exhibited the highest LPA production in *E. coli*.[32] Previously, a glucose dehydrogenase has also been utilized to increase the titer of LPA[61], dehydrogenase converts NADP to NADPH. NADPH is a substrate utilized by *dpkA* in the L-lysine α-oxidase pathway, meaning that increasing the concentration of the compound should increase the LPA production.

4.3 The effect of hydrogen peroxide on the L-lysine α-oxidase pathway

This study found considerable effect on the L-lysine α-oxidase pathway when supplementing or removing hydrogen peroxide from the bacterial culture. Increased hydrogen peroxide concentration resulted in an increased 5AVA titer, while removal of the compound increased the titer of LPA. This is in accordance with the previous study in *E. coli* where the supply of hydrogen peroxide led to an increased concentration of 5AVA when relying on spontaneous α-ketolysine conversion.[62] Contrary, increased catalase activity without the addition of hydrogen peroxide has increased the titer of 5AVA in *E. coli* when the enzymatic conversion of α-ketolysine to 5AVA was established instead of the spontaneous conversion in the presence of hydrogen peroxide.[63] This was presumably due to the omission of hydrogen peroxide toxicity that occurs when the spontaneous pathway is used. This indicates that the type of pathway used for conversion of α-ketolysine to 5AVA is critical when it comes to the necessity of hydrogen peroxide supply.

4.4 Future considerations

The L-lysine α-oxidase pathway utilizes L-lysine as its precursor. Therefore, increasing the L-lysine available will likely increase the metabolic flux through the pathway. The L-lysine permease (*lysP*) originating from *E. coli* has previously been utilized to improve LPA production in *E. coli* by increasing the L-lysine available in the cell.[61] Additionally, the L-lysine exporter (*lysE*) has previously been deleted in *C. glutamicum* to increase the production of LPA by increasing the concentration of L-lysine inside the cell.[64] Both approaches are encouraging and have the potential to be applied to *B. methanolicus* to increase the titers of both 5AVA and LPA.

L-lysine biosynthesis is regulated by feedback inhibition, meaning that an increased concentration of L-lysine in the cell leads to decreased production. This phenomenon has also been observed in *B. methanolicus*.[65] The same study investigated several genes connected to L-lysine feedback inhibition in classical mutants of *B. methanolicus* overproducing the compound and found mutations in the *lysA* and *dapG* genes. A reasonable approach to increase the titer of LPA and 5AVA will therefore be to repress these genes to increase the concentration of the key substrate of the L-lysine α-oxidase pathway. On the other hand, a metabolic pull mechanism was previously observed for cadaverine accumulation, indicating that rapid transformation of L-lysine to other intermediates prevents feedback inhibition.[66]

The repression of the L-lysine exporter and the genes associated with the feedback inhibition

of L-lysine synthesis can be achieved with the previously developed CRISPERi/Cas9 tool for *B. methanolicus*.[20] However when this tool was applied to repress the *katA* gene, only a 25 % reduction in activity was achieved. It is therefore suggested that a deletion tool is developed for *B. methanolicus*, as it possibly can increase the deactivation of genes associated with feedback inhibition of L-lysine, allowing for increased L-lysine concentrations in *B. methanloicus*. This tool would bolster the lackluster toolbox of the organism, easing studying of it in areas other than the L-lysine α-oxidase pathway as well.

To utilize *B. methanolicus* as an industrial organism producing 5AVA or LPA, it is eventually necessary to scale the cultures to larger fermenters. This will uncover possible problems associated with larger scales and help verify the results found in this study. Many of the results from this study exhibits significant uncertainties, which requires further testing. Therefore, verification of these results is needed as well.

5 Conclusion

The present study revealed for the first time the effect of hydrogen peroxide in the heterologous L-lysine α-oxidase pathway in *B. methanolicus*, towards methanol-based production of 5AVA and LPA. On the one hand, the presence of hydrogen peroxide led to the production of 21.41 $\pm$ 11.72 mg/l 5AVA in an engineered, hydrogen peroxide tolerant *B. methanolicus* strain. On the other hand, hydrogen peroxide removal by increased catalase activity led to the production of LPA that reached a titer of 17.14 $\pm$ 7.5 mg/l, leading to a proof of concept for the production of LPA in *B. methanolicus*.

This work opens doors for future strain development and investigation of the L-lysine α-oxidase pathway in *B. methanolicus*. Hydrogen peroxide has been identified as a key factor in the production of 5AVA and LPA. This study has shed light on some of its effects when producing the compounds. Critical aspects of 5AVA and LPA production in *B. methanolicus* has also been illuminated, such as the toxicity of the compounds and the impact of induction time on the production.

References

[1] F. J. Schendel, C. E. Bremmon, M. C. Flickinger, M. Guettler, and R. S. Hanson. L-lysine production at 50 degrees c by mutants of a newly isolated and characterized methylotrophic *Bacillus sp.* *Applied and Enviornmental Microbiology*, 2009. doi: 10.1128/aem.56.4.963-970.1990. URL `https://journals.asm.org/doi/abs/10.1128/aem.56.4.963-970.1990`.

[2] T. Brautaset, Ø. M. Jakobsen, K. D. Josefsen, M. C. Flickinger, and T. E. Ellingsen. *Bacillus methanolicus*: a candidate for industrial production of amino acids from methanol at 50 degrees c. *Appl Microbiol Biotechnol*, 1992. doi: 10.1007/s00253-006-0757-z. URL `https://pubmed.ncbi.nlm.nih.gov/17216461/`.

[3] Ba. Delépine, M. G. López, M. Carnicer, C. M. Vicente, V. F. Wendisch, S. Heux, and M. Liebeke. Charting the metabolic landscape of the facultative methylotroph *Bacillus methanolicus*. *mSystems*, 2020. doi: 10.1128/mSystems.00745-20. URL `https://journals.asm.org/doi/10.1128/mSystems.00745-20`.

[4] M. Irla, A. Neshat, A. Winkler, A. Albersmeier, T. M. Heggeset, T. Brautaset, J. Kalinowski, V. F. Wendisch, and C. Rückert. Complete genome sequence of *Bacillus methanolicus* mga3, a thermotolerant amino acid producing methylotroph. *Journal of biotechnology,*, 2014. URL `https://pubmed.ncbi.nlm.nih.gov/25152427/,DOI={10.1016/j.jbiotec.2014.08.013}`.

[5] J. E. Müller, B. Litsanov, M. Bortfeld-Miller, C. Trachsel, J. Grossmann, and T. Brautaset. Proteomic analysis of the thermophilic methylotroph *Bacillus methanolicus* MGA3. *Proteomics*, 2014. doi: 10.1002/pmic.201300515. URL `https://pubmed.ncbi.nlm.nih.gov/24452867/`.

[6] M. Irla, A. Neshat, T. Brautaset, C. Rückert, J. Kalinowski, and Wendisch. Transcriptome analysis of thermophilic methylotrophic *Bacillus methanolicus* MGA3 using RNA-sequencing provides detailed insights into its previously uncharted transcriptional landscape. *BMC genomics*, 2015. doi: /10.1186/s12864-015-1239-4. URL `https://pubmed.ncbi.nlm.nih.gov/25758049/`.

[7] M. Carnicer, G. Vieira, and T. Brautaset. Quantitative metabolomics of the thermophilic methylotroph *Bacillus methanolicus*. *Microbial Cell Factories*, 2016. doi: 10.1186/s12934-016-0483-x. URL `https://microbialcellfactories.biomedcentral.com/articles/10.1186/s12934-016-0483-x#citeas`.

[8] N. Arfman, E. M. Watling, and W Clement. Methanol metabolism in thermotolerant methylotrophic *Bacillus* strains involving a novel catabolic nad-dependent methanol dehydrogenase as a key enzyme. 1989. doi: 10.1007/BF00409664. URL `https://link.springer.com/article/10.1007/BF00409664`.

[9] T. M. Heggeset, A. Krog, S. Balzer, A. Wentzel, T. E. Ellingsen, and T. Brautaset. Genome sequence of thermotolerant *Bacillus methanolicus*: features and regulation related to methylotrophy and production of l-lysine and l-glutamate from methanol. *Appl Environ Microbiol*, 2012. doi: 10.1128/AEM.00703-12. URL `https://pubmed.ncbi.nlm.nih.gov/22610424/`.

[10] T. Brautaset, Ø. M. Jakobsen, and K. F. Degnes. *Bacillus methanolicus* pyruvate carboxylase and homoserine dehydrogenase i and ii and their roles for l-lysine production from methanol at 50 degrees c. *Appl Microbiol Biotechnol*, 2010. doi: 10.1007/s00253-010-2559-6. URL `https://pubmed.ncbi.nlm.nih.gov/20372887/`.

[11] M. Irla, T. M. B. Heggeset, I. Nærdal, L. Paul, T. Haugen, S. B. Le, T. Brautaset, and V. F. Wendisch. Genome-based genetic tool development for *Bacillus methanolicus*: Theta- and rolling circle-replicating plasmids for inducible gene expression and application to methanol-based cadaverine production. *Frontiers in Microbiology*, 2016.

doi: 10.3389/fmicb.2016.01481. URL https://www.frontiersin.org/article/10.3389/fmicb.2016.01481.

[12] L. F. Brito, M. Irla, I. Nærdal, S. B. Le, B. Delépine, St. Heux, and T. Brautaset. Evaluation of heterologous biosynthetic pathways for methanol-based 5-aminovalerate production by thermophilic *Bacillus methanolicus*. *Frontiers in Bioengineering and Biotechnology*, 2021. doi: 10.3389/fbioe.2021.686319. URL https://www.frontiersin.org/article/10.3389/fbioe.2021.686319.

[13] M. Irla, I. Nærdal, T. Brautaset, and V. F. Wendisch. Methanol-based γ-aminobutyric acid (gaba) production by genetically engineered *Bacillus methanolicus* strains. *Industrial Crops and Products*, 2017. doi: 10.1016/j.indcrop.2016.11.050. URL https://www.sciencedirect.com/science/article/pii/S0926669016308135.

[14] E. B. Drejer, D. T. C. Chan, C. Haupka, V. F. Wendisch, T. Brautaset, and M. Irla. Methanol-based acetoin production by genetically engineered *Bacillus methanolicus*. *Green Chem.*, 2020. doi: 10.1039/C9GC03950C. URL http://dx.doi.org/10.1039/C9GC03950C.

[15] S. Hakvåg, In. Nærdal, T. M. B. Heggeset, K. A. Kristiansen, I. M. Aasen, and T. Brautaset. Production of value-added chemicals by *Bacillus methanolicus* strains cultivated on mannitol and extracts of seaweed saccharina latissima at 50°c. *Frontiers in Microbiology*, 2020. doi: 10.3389/fmicb.2020.00680. URL https://www.frontiersin.org/article/10.3389/fmicb.2020.00680.

[16] N. Arfman, E. M. Watling, W. Clement, R. J. van Oosterwijk, G. E. de Vries, W. Harder, M. M. Attwood, and L. Dijkhuizen. Methanol metabolism in thermotolerant methylotrophic *Bacillus* strains involving a novel catabolic nad-dependent methanol dehydrogenase as a key enzyme. *Archives of Microbiology*, 1991. doi: 10.1007/BF00409664. URL https://www.sciencedirect.com/science/article/pii/S0926669016308135.

[17] H. Yurimoto, N. Kato, and Y. Sakai. Genomic organization and biochemistry of the ribulose monophosphate pathway and its application in biotechnology. *Appl Microbiol Biotechnol*, 2009. doi: 10.1007/s00253-009-2120-7. URL https://link.springer.com/article/10.1007/s00253-009-2120-7.

[18] C. A. R. Cotton, N. J. Claassens, S. Benito-Vaquerizo, and A. Bar-Even. Renewable methanol and formate as microbial feedstocks. *Current Opinion in Biotechnology*, 2020. doi: https://doi.org/10.1016/j.copbio.2019.10.002. URL https://www.sciencedirect.com/science/article/pii/S0958166919301004. Energy Biotechnologyy Environmental Biotechnology.

[19] Ø. M. Jakobsen, A. Benichou, M. C. Flickinger, S. Valla, T. E. Ellingsen, and T. Brautaset. Upregulated Transcription of Plasmid and Chromosomal Ribulose Monophosphate Pathway Genes Is Critical for Methanol Assimilation Rate and Methanol Tolerance in the Methylotrophic Bacterium *Bacillus methanolicus*. 2006. doi: 10.1128/JB.188.8.3063-3072.2006. URL https://www.ncbi.nlm.nih.gov/pmc/articles/PMC1446977/.

[20] K. Schultenkämper, L. F. Brito, and M. López. Establishment and application of CRISPR interference to affect sporulation, hydrogen peroxide detoxification, and mannitol catabolism in the methylotrophic thermophile *Bacillus methanolicus*. *Appl Microbiol Biotechnol*, 2019. doi: 10.1007/s00253-019-09907-8. URL https://link.springer.com/article/10.1007%2Fs00253-019-09907-8#citeas.

[21] J. Schrader, M. Schilling, D. Holtmann, D. Sell, M. Villela Filho, A. Marx, and J. A. Vorholt. Methanol-based industrial biotechnology: current status and future perspectives of methylotrophic bacteria. *Trends in Biotechnology*, 2009. doi: https://doi.org/10.1016/j.tibtech.2008.10.009. URL https://www.sciencedirect.com/science/article/pii/S0167779908002898.

[22] Biomass yield on glucose. URL https://bionumbers.hms.harvard.edu/bionumber.aspx?s=n&v=6&id=108126. Accessed: 31.05.2022.

[23] V. F. Wendisch. Metabolic engineering advances and prospects for amino acid production. *Metabolic engineering*, 2020. doi: 10.1016/j.ymben.2019.03.008. URL https://pubmed.ncbi.nlm.nih.gov/30940506/.

[24] Biotechnology market size, share trends analysis report. URL https://www.grandviewresearch.com/industry-analysis/biotechnology-market. Accessed: 26.05.2022.

[25] Yu JH Hyun SM Khang TU Kang KH Song BK Park K Oh MK Lee SY Park SJ Joo JC, Oh YH. Production of 5-aminovaleric acid in recombinant corynebacterium glutamicum strains from a miscanthus hydrolysate solution prepared by a newly developed miscanthus hydrolysis process. *Bioresour Technol*, 2017. doi: 10.1016/j.biortech.2017.05.131. URL https://pubmed.ncbi.nlm.nih.gov/28579174/.

[26] Xin Wang, Peipei Cai, Kequan Chen, and Pingkai Ouyang. Efficient production of 5-aminovalerate from l-lysine by engineered escherichia coli whole-cell biocatalysts. *Journal of Molecular Catalysis B: Enzymatic*, 2016. doi: 10.1016/j.molcatb.2016.10.008. URL https://www.sciencedirect.com/science/article/pii/S1381117716302016.

[27] C. Haupka, L. F. Brito, T. Busche, D. Wibberg, and V. F. Wendisch. Genomic and transcriptomic investigation of the physiological response of the methylotroph *Bacillus methanolicus* to 5-aminovalerate. *Front Microbiol*, 2021. doi: 10.3389/fmicb.2021.664598. URL https://www.ncbi.nlm.nih.gov/pmc/articles/PMC8119775/.

[28] 5-aminovaleric acid. URL shorturl.at/hEGLX. Accessed: 31.05.2022.

[29] L. A. Watanabe, S. Haranaka, B. Jose, M. Yoshida, T. Kato, M. Moriguchi, K. Soda, and N. Nishino. An efficient access to both enantiomers of pipecolic acid. *Tetrahedron: Asymmetry*, 2005. doi: 10.1016/j.tetasy.2005.01.017. URL https://www.sciencedirect.com/science/article/pii/S0957416605000583.

[30] T. Fujii, M. Mukaihara, H. Agematu, and H. Tsunekawa. Biotransformation of l-lysine to l-pipecolic acid catalyzed by l-lysine 6-aminotransferase and pyrroline-5-carboxylate reductase. *Bioscience, Biotechnology, and Biochemistry*, 2002. doi: 10.1271/bbb.66.622. URL https://www.jstage.jst.go.jp/article/bbb/66/3/66_3_622/_article/-char/ja/.

[31] He M. Pipecolic acid in microbes: biosynthetic routes and enzymes. *Journal of industrial microbiology biotechnology*, 2006. doi: 10.1007/s10295-006-0078-3. URL https://pubmed.ncbi.nlm.nih.gov/16418868/.

[32] X. Xu, Z. Rao, J. Xu, and W. Zhang. Enhancement of l-pipecolic acid production by dynamic control of substrates and multiple copies of the pipa gene in the escherichia coli genome. *ACS Synthetic Biology*, 2022. doi: 10.1021/acssynbio.1c00467. URL https://doi.org/10.1021/acssynbio.1c00467.

[33] F. Pérez-García, P. Peters-Wendisch, and Volker F. Wendisch. Engineering Corynebacterium glutamicum for fast production of L-lysine and L-pipecolic acid. *Applied Microbiology and Biotechnology*, 2016. doi: 10.1007/s00253-016-7682-6. URL https://link.springer.com/article/10.1007/s00253-016-7682-6#citeas.

[34] L-pipecolic acid. URL https://www.sigmaaldrich.com/NO/en/product/sigma/p2519. Accessed: 19.11.2020.

[35] Y. Tani, R. Miyake, and R Yukami. Functional expression of l-lysine -oxidase from *Scomber japonicus* in *Escherichia coli* for one-pot synthesis of l-pipecolic acid from dl-lysine. *Appl Microbiol Biotechnol*, 2015. doi: 10.1007/s00253-014-6308-0. URL https://link.springer.com/article/10.1007/s00253-014-6308-0#citeas.

[36] A. V. Pukin, C. G. Boeriu, E. L. Scott, J. P.M. Sanders, and M. C. R. Franssen. An efficient enzymatic synthesis of 5-aminovaleric acid. *Journal of Molecular Catalysis B: Enzymatic*, 2010. doi: 10.1016/j.molcatb.2009.12.006. URL https://www.sciencedirect.com/science/article/pii/S1381117709003105.

[37] H. Aebi. Catalase. In Hans Ulrich Bergmeyer, editor, *Methods of Enzymatic Analysis (Second Edition)*. Academic Press, 1974. doi: https://doi.org/10.1016/B978-0-12-091302-2.50032-3. URL https://www.sciencedirect.com/science/article/pii/B9780120913022500323.

[38] C. C. Winterbourn. The biological chemistry of hydrogen peroxide. methods in enzymology. 2013. doi: 10.1371/journal.pone.0091813. URL 10.1016/B978-0-12-405881-1.00001-X.

[39] E. J. Calabrese and A. T. Canada. Catalase: Its role in xenobiotic detoxification. *Pharmacology Therapeutics*, 1989. doi: 10.1016/0163-7258(89)90069-7. URL https://www.sciencedirect.com/science/article/pii/0163725889900697.

[40] L. F. Brito. Unpublished work. 2017-2021.

[41] B. Skagestad. Assessing catalase activity in *Bacillus methanolicus*: A prerequisite for methanol-based l-pipecolic acid production. *NTNU*, 2021.

[42] D. Hanahan. Studies on transformation of *Escherichia coli* with plasmids. 1983. doi: 10.1016/s0022-2836(83)80284-8. URL https://pubmed.ncbi.nlm.nih.gov/6345791/.

[43] C. Haupka. Metabolic engineering of methylotrophic *Bacillus methanolicus* and non-methylotrophic corynebacterium glutamicum for production of lysine-derived compounds. 2021. URL https://pub.uni-bielefeld.de/record/2956967.

[44] P. Puigbò, E. Guzmán, A. Romeu, and S. Garcia-Vallvé. OPTIMIZER: a web server for optimizing the codon usage of DNA sequences. *Nucleic Acids Research*, 2007. doi: 10.1093/nar/gkm219. URL https://doi.org/10.1093/nar/gkm219.

[45] Biotium. Gelred® nucleic acid gel stain, (downloaded 27.05.2022). URL https://biotium.com/product/gelred-nucleic-acid-gel-stain/.

[46] Thermo Fisher Scientific. Dna gel loading dye (6x), (downloaded 27.05.2022). URL https://www.thermofisher.com/order/catalog/product/R0611.

[47] New England Biolabs. 1 kb plus dna ladder, (downloaded 08.06.2022). URL https://international.neb.com/products/n3200-1-kb-plus-dna-ladder#Product%20Information.

[48] Sci Ed Software. Clone manager 10, basic edition, (downloaded 26.11.2021). URL https://www.scied.com/pr_cmbas.htm.

[49] Promega. Gotaq® g2 dna polymerase, (downloaded 27.05.2022). URL https://no.promega.com/products/pcr/taq-polymerase/gotaq-g2-dna-polymerase/?catNum=M7841.

[50] Takara. Cloneamp hifi pcr premix—high-fidelity pcr for cloning, (downloaded 27.05.2022). URL https://www.takarabio.com/products/pcr/pcr-master-mixes/high-fidelity/cloneamp-hifi-pcr-premix.

[51] Eppendorf. Mastercycler® nexus x2 - pcr thermal cycler, (downloaded 27.05.2022). URL https://www.eppendorf.com/no-en/eShop-Products/PCR/Cyclers/Mastercycler-nexus-X2-p-PF-82586.

[52] D. G. Gibson, L. Young, R. Y. Chuang, C. A. Venter, J. C.and Hutchison, 3rd, and H. O. Smith. Enzymatic assembly of DNA molecules up to several hundred kilobases. *Nature*

methods, 2009. doi: 10.1038/nmeth.1318. URL https://pubmed.ncbi.nlm.nih.gov/19363495/.

[53] Qiuagen. Qiaquick pcr purification kit, (downloaded 27.05.2022). URL https://www.qiagen.com/us/products/discovery-and-translational-research/dna-rna-purification/dna-purification/dna-clean-up/qiaquick-pcr-purification-kit/.

[54] Zymo. Instruction manual, (downloaded 26.10.2021). URL https://fnkprddata.blob.core.windows.net/domestic/data/datasheet/ZYR/D4209.pdf.

[55] T. Haas, M. Poetter, J. C. Pfeffer, W. Kroutil, A. Skerra, and A. Lerchner. Oxidation and amination of secondary alcohols. *European Patent Office*, 2014. URL https://patents.google.com/patent/US20140308717A1/en.

[56] Waters. 2475 fluorescence (flr) detector, (downloaded 26.10.2021). URL https://www.waters.com/waters/en_US/2475-Fluorescence-%28FLR%29-Detector/nav.htm?cid=514434&locale=en_US.

[57] Waters. Symmetry c18 column, (downloaded 25.05.2022). URL https://www.waters.com/nextgen/no/en/shop/columns/wat066224-symmetry-c18-column-100a-35--m-46-mm-x-75-mm-1-pk.html.

[58] Waters. waters e2695 seperation modules, (downloaded 26.05.2022). URL https://www.waters.com/webassets/cms/library/docs/720002552en.pdf.

[59] L. Fowden and M.H. Richmond. Replacement of proline by azetidine-2-carboxylicacid during biosynthesis of protein. *Biochimica et Biophysica Acta*, 1963. doi: 10.1016/0006-3002(63)91104-1. URL https://www.sciencedirect.com/science/article/pii/0006300263911041.

[60] M. H. Zwietering, I. Jongenburger, F. M. Rombouts, and K. van 't Riet. Modeling of the bacterial growth curve. *Applied and enviornmental microbiology*, 1990. doi: 10.1128/aem.56.6.1875-1881.1990. URL https://www.ncbi.nlm.nih.gov/pmc/articles/PMC184525/.

[61] J. Cheng, Y. Huang, L. Mi, W. Chen, D. Wang, and Q. Wang. An economically and environmentally acceptable synthesis of chiral drug intermediate l-pipecolic acid from biomass-derived lysine via artificially engineered microbes. *J Ind Microbiol Biotechnol*, 2018. doi: 10.1007/s10295-018-2044-2. URL https://academic.oup.com/jimb/article/45/6/405/5996738.

[62] J. Cheng, W. Tu, Z. Luo, L. Liang, X. Gou, X. Wang, C. Liu, and G. Zhang. Co-production of 5-aminovalerate and γ-valerolactam for the synthesis of nylon 5 from l-lysine in escherichia coli. *Frontiers in Bioengineering and Biotechnology*, 2021. doi: 10.3389/fbioe.2021.726126. URL https://www.frontiersin.org/article/10.3389/fbioe.2021.726126.

[63] J. Cheng, W. Tu, and Z. Luo. A high-efficiency artificial synthetic pathway for 5-aminovalerate production from biobased l-lysine in escherichia coli. *Front Bioeng Biotechnol.*, 2021. doi: 10.3389/fbioe.2021.633028. URL https://www.ncbi.nlm.nih.gov/pmc/articles/PMC7900509/.

[64] F. Pérez-García, J. Max Risse, K. Friehs, and V. F. Wendisch. Fermentative production of l-pipecolic acid from glucose and alternative carbon sources. *Biotechnology Journal*, 2017. doi: https://doi.org/10.1002/biot.201600646. URL https://onlinelibrary.wiley.com/doi/abs/10.1002/biot.201600646.

[65] I. Nærdal, Netzer R., T. E. Ellingsen, and T. Brautaset. Analysis and manipulation of aspartate pathway genes for l-lysine overproduction from methanol by *Bacil-*

lus methanolicus. *Appl Environ Microbiol*, 2011. doi: 10.1128/AEM.05093-11. URL https://pubmed.ncbi.nlm.nih.gov/21724876/.

[66] I. Naerdal, J. Pfeifenschneider, T. Brautaset, and V. F. Wendisch. Methanol-based cadaverine production by genetically engineered *Bacillus methanolicus* strains. *Microbial biotechnology*, 2015. doi: 10.1111/1751-7915.12257. URL https://www.ncbi.nlm.nih.gov/pmc/articles/PMC4353347/.

[67] R. Green and E. J. Rogers. Transformation of chemically competent e. coli. *Methods Enzymol*, 2011. doi: 10.1016/B978-0-12-418687-3.00028-8. URL https://www.ncbi.nlm.nih.gov/pmc/articles/PMC4037286/.

A Growth media and buffers

The media and buffers utilized in this study are presented in this section. All solutions were autoclaved at 121 °C for 20 minutes. All the chemicals used in this study were purchased from Sigma Aldrich unless stated otherwise.

A.1 SOB medium

Table A.1: SOB medium composition.

Compound	Amount
Hannah's blend	28 g/l
Deionized water	To 1 l

If preparing an agar plate, 15g/l bacterial agar was added.

A.2 LB medium

Table A.2: LB medium composition.

Compound	Amount
Tryptone	10 g/l
Yeast extract	5 g/l
Sodium chloride	5 g/l
Deionized water	To 1 l

If preparing an agar plate, 15g/l bacterial agar was added.

A.3 MvcM High Salt Buffer 10x

Table A.3: MVcM High Salt Buffer 10x composition

Compound	Amount
K_2HPO_4	41.0 g/l
NaH_2PO_4	15.0 g/l
$(NH_4)_2SO_4$	21.2 g/l
Deionized water	To 1 l

A.4 MvcMy medium

Table A.4: MVcMY medium composition

Compound	Amount
MVcM High Salt Buffer 10x	100 ml/l
Deionized water	890.00 l
Yeast extract	0.25 g/l
Vitamins*	1.00 ml/l
Trace metals*	1.00 ml/l
Methanol (> 99.98 %)	8.11 ml/l
$MgSO_4$ (1 M)	1.00 ml/l

* vitamins and trace metals are prepared as per a previous study [12].

A.5 MvcM medium

Table A.5: MVcM medium composition

Compound	Amount
MvCM High Salt Buffer 10x	100 ml/l
Deionized water	890.00 l
Vitamins*	1.00 ml/l
Trace metals*	1.00 ml/l
Methanol (> 99.98 %)	8.11 ml/l
$MgSO_4$ (1 M)	1.00 ml/l

* vitamins and trace metals are prepared as per a previous study [12].

A.6 Tris-Acetate-EDTA buffer

Table A.6: 50 X Tris-Acerate-EDTA buffer

Compound	Amount
Tris Base (2 M)	242 g
Acetic acid	57.1 ml
EDTA pH 8 (0.5 M)	100 ml
Deionized water	To 1 l

A.7 Glycerol solution

Table A.7: Glycerol solution

Compound	Amount
> 99 % glycerol	200 ml
Milliq water	200 ml

A.8 TfBI

Table A.8: TfBII, table adapted from previous study.[67] Filter sterilize after mix is complete.

Compound	Amount
Potassium acetate	1.18 g/400 ml
$RbCl_2$ water	4.84 g/400 ml
$CaCl_2 \cdot 2H_2O$	0.59 g/400 ml
$MnCl_2$	3.96 g/400 ml
glycerol	60 ml/400 ml
Acetic acid	until pH 5.8
MilliQ water	until 400 ml

A.9 TfBII

Table A.9: TfBI, recipe adapted from previous study.[67] Filter sterilize after mix is complete.

Compound	Amount
MOPS	0.21 g/100 ml
$CaCl_2 \cdot 2H_2O$	1.1 g/100 ml
$RbCl_2$ water	0.12 g/100 ml
glycerol	15 ml/100 ml
NaOH	until pH 6.5
MilliQ water	until 100 ml

A.10 1 kb NEB DNA ladder

Table A.10: 1 kb DNA ladder[47]

Compound	Amount
Water	4 parts
DNA Ladder	1 part
6X DNA loading dye	1 part

B Construction of pUB110Smp-*katA*

An attempt to create a higher compy number plasmid to increase the activity of catalase was attempted. This was to be achieved with the insertion of the homologous *katA* gene into pUB110Smp. The digestion of the pUB110Smp was attempted, and the resulting gel electrophoresis image is shown in Figure B.1.

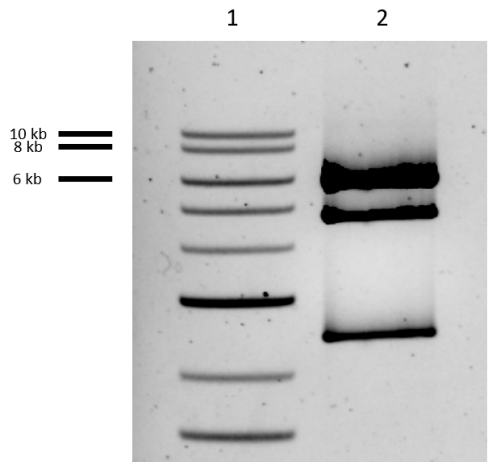

Figure B.1: Agarose gel electrophoresis image of digested pUB110Smp plasmid. Well 1 shows the DNA ladder. Well 2 shows pUB110Smp digested by PciI.

There are three bands present in the gel electrophoresis image resulting from the digestion of pUB110Smp plasmid seen in B.1. This digestion was attempted multiple times, however, it was unsuccessful each time. The likely reason is mutations in the plasmid, although sequencing of the entire plasmid is needed to confirm this.

C DNA sequencing results

Due to the large amount of sequencing data, only a part of the sequence will be displayed in this section.

C.1 pBV2xp-*aip*^{SjBi}-*dpkA*^{Ps}

```
1           CAGGAATGGCAGGATTAACAGCAGCAAAATTATTACTAGATGCAGGACATACAGTTACAA
2           TATTACGCCAGCTGGCGAAAGGGGGATGTGCTGCAAGGCGATTAAGTTGGGTAACGCCAG
3           CACGATCTTTATTAATTGATAAAGCAAGATCTGCAGGAGTTGCAATTTTAGCAATTATAG
plasmid     CAAGATCTTTATTAATTGATAAAGCAAGATCTGCAGGAGTTGCAATTTTAGCAATTAGAG


1           TTTTATAAGCAAATGATAGAGTTGGAGGAAGA-GTTGAAACATATAGAAATGAAAAAGAA
2           GGT--TTTCCCAGTCACGACGTTGTAAAACGACGGCCAGTGAATTCGAGCTCATGGTACG
3           GATC-TCATCATTTTGCAGCATTATGGCCAGATGTTGAACCATTTGCAGAACAAGGATTA
plasmid     GATC-TCATCATTTTGCAGCATTATGGCCAGATGTTGAACCATTTGCAGAACAAGGATTA


1           GGATGGTATGCAGAAATGGGAGCAATGAGAATTCCATCTTCTCATAGAATTGTTCAATGG
2           GATCTTAATGTCCTGCTAATTCTTGTAATCTTTCTAAATCTGCTTGTGCAATAACAATT-
3           CTTGCTTTATCTATGGTTAATTCTATGACATGTGTTGTTCCACATGGAGCAAGACAACCA
plasmid     GTTGCATTATCTATGGTTAATTCTATGACATGTGTTGTTCCACATGGAGCAAGACAACCA


1           TTTGTTAAAAAATTAGGAGTTGAAATGAATGAATTTGTTATGACAGATGATAATACATTT
2           CCATGTGCCATAGATCTTGCT-CTTTCTAAATATCTT--CTATCTCCTGGTAATCTTTCT
3           TTATTTGGAACAAATCCAATTGCATTTGGAGCACCAA--GAGCAGGAGGAGAACCAATTG
plasmid     TTATTTGGAACAAATCCAATTGCATTTGGAGCACCAA--GAGCAGGAGGAGAACCAATTG


1           TATTTAGTT-AATGGAGTT---AGAGAAAGAACATATGTTGTTCAAGAAAATCCAGATGT
2           TGTCCAACTCCATGTAATTGTCTAACTAATTCTTCAGATCTTTGTGCAAAATGTTGTCCT
3           TTTTTGATT-TA-GCAACA---TCTGCAATTGCACATGGAGATGTTCAAATTGCAG-CAA
plasmid     TTTTTGATT-TA-GCAACA---TCTGCAATTGCACATGGAGATGTTCAAATTGCAG-CAA


1           TTTAAAATATAATGTTTCTGAATCTGAAAAAGGAATTTCTGCAGATGATTTATTAGATAG
2           GCTCCTTTATCTGGATCAAT-AACAATTAATAATTGTCCTGTCCATGGTGTTTGTGCTCC
3           GAGAAGGAAGATTATTACC--AGCAGGAATGGGAGTTGATAGAGATGGATTACCAACACA
plasmid     GAGAAGGAAGATTATTACC--AGCAGGAATGGGAGTTGATAGAGATGGATTACCAACACA


1           AGCATTACAAAAAGTTAAAGAAGAAGTTGAAGCAAATGGATGTAAAGCAGCATTAGAAAA
2           TGGATGTTTAGACCAATCAAATTCAAAAGAAAAATTTCCTCCTGTTAAT-CCTGCTGCTA
3           AGAACCAAGAGCAATTTTAGATGGAGGAGCATTATTACCATTTGGAGGA-CATAAAGGAT
plasmid     AGAACCAAGAGCAATTTTAGATGGAGGAGCATTATTACCATTTGGAGGA-CATAAAGGAT


1           ATATGATAGATATTCT-GTTAAAGAATATTTAAAAGA---AGAAGGAGGATTATCTCCAG
2           ATAATTCAACCATCATAGATAATGCAGATCCTTTATGTCCTCCAAATGGTAATAATGCTC
3           CTGCATTATCTATGATGGTTGAATTATTAGCAGCAGGATTAACAGGAGGAAATTTTTCTT
plasmid     CTGCATTATCTATGATGGTTGAATTATTAGCAGCAGGATTAACAGGAGGAAATTTTTCTT


1           GAGCAGTTAGAATGATTGGAGATTTATTAAATGAACAATCTTTAATGTATACAGCATTAT
2           CTCCATCTAAAATTGCTCTTGGTTCTTGTGTTGGTAATCCATCTCTATCAACTCCCATTC
3           TTGAATTTGATTGGTCTAAACATCCAGGAGCACAAACACCATGGACAGGACAATTATTAA
plasmid     TTGAATTTGATTGGTCTAAACATCCAGGAGCACAAACACCATGGACAGGACAATTATTAA


1           CTGAAATGATTTATGATCAAGCAGATGTTAATGATTCTGT------TTCTTATCATGAAG
2           CTGCTGGTAATAATCTTCCTTCTCTTG--CTGCAATTTGAAC----ATCTCCATGTGCAA
3           TTGTTATTGATCCAGATAAAGGAGCAGGACAACATTTTGCACAAAGATCTGAAGAATTAG
plasmid     TTGTTATTGATCCAGATAAAGGAGCAGGACAACATTTTGCACAAAGATCTGAAGAATTAG
```

Figure C.1: Sequencing results for positive pBV2xp-*aip*^{SjBi}-*dpkA*^{Ps}. Part 1. 1, 2, and 3 indicates the different sequencign results, while plasmid is the theoretical plasmid.

```
1           TTACAGGAGGATCTGATTTATTACCAGAAGCATTTTTATCTGTTTTAGATGTTCCAATTT
2           TTGCAGATGTTGCTAAATCAAAAACAATTGGTTCTCCTCCTGCTCTTGGTGCTCCAAATG
3           TTAGACAATTACATGGAGTTGGACAAGAAAGATTACCAGGAGATAGAAGATATTTAGAAA
plasmid     TTAGACAATTACATGGAGTTGGACAAGAAAGATTACCAGGAGATAGAAGATATTTAGAAA

1           TATTAAATTCTAAAG----TTAAACA--TATTAGACAATCTGAT--AAAGGAGTTATTGT
2           CAATTGGATTTGTTCCAAATAATGGTTGTCTTGCTCCATGTGGAACAACACATGTCATAG
3           GAGCAAGATCTATGGCACATGGAATTGTTATTGCACAAGCAGATTTAGAAAGATTACAAG
plasmid     GAGCAAGATCTATGGCACATGGAATTGTTATTGCACAAGCAGATTTAGAAAGATTACAAG

1           TTCTTATCAAACAGGAA--ATGAATCTTCTTTAATGGATTTATCTGCAGATATTGTTTTA
2           AATTAACCATAGATAATGCAACTAATCCTTGTTCTGCAAATGGTTCAACATCTGGCCATA
3           AATTAGCAGGACATTAAG-ATCCGTACCATGAGCTCGAATTCACTGGCCGTCGTTTTACA
plasmid     AATTAGCAGGACATTAAG-ATCCGTACCATGAGCTCGAATTCACTGGCCGTCGTTTTACA

1           GTTACA-ACAACAGCAAAAGC--AGCATT-----ATTTATTGATTTTGATCCACCATTAT
2           ATGCTGCAAAATGATGAGATCCTCTAATTGCTAAAATTGCAACTCCTGCAG---ATCTTG
3           ACGTCG-TGACTGGGAAAACCCTGGCGTTACCCAACTTAATCGCCTTGCAGCACATCCCC
plasmid     ACGTCG-TGACTGGGAAAACCCTGGCGTTACCCAACTTAATCGCCTTGCAGCACATCCCC

1           CTATTTCTAAATGGAAGCATTAAGATCTGTTCATT-ATGATTCTTCTA------------
2           CTTTATCAATTAATAAAGATCTTGCTGCTGCTAATGCTGGTTGTGCAAATCCA-------
3           CTTTCGC-AGCTGGCGTAATAGCGAAGAGGCCCGC-CCGATCGCCCTT------------
plasmid     CTTTCGCCAGCTGGCGTAATAGCGAAGAGGCCCGCACCGATCGCCCTTCCCAACAGTTGC
```

Figure C.2: Sequencing results for positive pBV2xp-aip^{SjBi}-$dpkA^{Ps}$. Part 2. 1, 2, and 3 indicates the different sequencign results, while plasmid is the theoretical plasmid.

The sequencing results shown in Figure C.1 and Figure C.2 shows that pBV2xp-aip^{SjBi}-$dpkA^{Ps}$ has been constructed correctly.

C.2 pBV2xp-*aip*^{SjBi}-*dpkA*^{Pp}

```
1           -TTGAAATAAACATTTATTTTGTATATGATGAGATAAAGTTAGTTTATTGGATAAACAAA
2           --TCATTTACAGAATTACAATCTTTATTACAAG---CAATTTTTCAAAGACATGGATGTT
3           -GCGATCGGTGCGGGCCTCTTCGCTATTACGC----CAGCTGGCGAAAGGGGGATGTGCT
plasmid     TTCCATTTACAGAATTACAATCTTTATTACAAG---CAATTTTTCAAAGACATGGATGTT

1           CTAACTCAATTAAGATAGTTGATGGATAAACTTGTTCACTTAAGGGGGAAATGGCTATGG
2           CTGAAGCAGTTGCAAGAGTTTTAGCACATAATTGTGCATCT---GCACAAAGAGATGGAG
3           GCAAGGCGATTAAGTTGGGTAACGCCAGGGTTTTCCCAGTCACGACGTTGTAAAACGACG
plasmid     CTGAAGCAGTTGCAAGAGTTTTAGCACATAATTGTGCATCT---GCACAAAGAGATGGAG

1           AACATT-TAGCAGATTGTTTAGAAGATAAAGA--TTATGATACATTATTACAAACATTAG
2           CACATTCTCATGGAGTTTTTAGAATGCCAGGATATGTTTCTACATTAGCATCTGGATGGG
3           GCCAGT---GCCAAGCTCTAGCGCCATTCGCCATTCAGGCTGCGCAACTGTTGGGAAGGG
plasmid     CACATTCTCATGGAGTTTTTAGAATGCCAGGATATGTTTCTACATTAGCATCTGGATGGG

1           ATAATGGAT------TACCACATAT------TAATACATCTCATCATGTTGTTATTGTTG
2           TTGATGGACAAGCAACACCACAAGTTTCTGATGTTGCAGCAGGATATGTTAGAGTTGATG
3           -CGATCGGTGCGGGCCTCTTCGCTAT-----TACGCCAGCTGGCGAAAGGGGGAT--GTG
plasmid     TTGATGGACAAGCAACACCACAAGTTTCTGATGTTGCAGCAGGATATGTTAGAGTTGATG

1           GAGCAGGAATGG---------CAGGATTAACAGCAGCAAAATTATTACAAGAT------G
2           CAGCAGGAGGATTTGCACAACCAGCATTAGCAGCAGCAAGAGAATTATTAGTTGCAAAAG
3           CTGCAAGGCGAT---------TAAGTTGGGTAAC-GCCAGGGTTTTCCCAGTCACGACGT
plasmid     CAGCAGGAGGATTTGCACAACCAGCATTAGCAGCAGCAAGAGAATTATTAGTTGCAAAAG

1           CAGGACATACAG---TTACAATTTTAGAAGCAAATGATA-----GAGTTGGAGGAAGAGT
2           CAAGATCTGCAGGAATTGCAGTTTTAGCAATTCATAATTCTCATCATTTTGCAGCATTAT
3           TGTAAAACGACGGCCAGTGAATTCGAGCTCATGGTACGGATC-TTATCCTAATAATTCTT
plasmid     CAAGATCTGCAGGAATTGCAGTTTTAGCAATTCATAATTCTCATCATTTTGCAGCATTAT

1           TGAAACATATAGAAA----TGAAAAAGAAGGATGGTATGCAGAAATGGGAG------CAA
2           GGCCAGATGTTGAACCATTTGCAGAAGAAGGATTAGTTGCATTATCTGTTGTTAATTCTA
3           TTAATCCTTTTAATTCTTGTTCTGTAACTGCAACTCCTTCTTCTTCTGCAACTTCTCTTT
plasmid     GGCCAGATGTTGAACCATTTGCAGAAGAAGGATTAGTTGCATTATCTGTTGTTAATTCTA

1           TGAGAATTCCATCTTCTCATAGA------ATTGTTCAATGGTTTGTTAAAAA--------
2           TGACATGTGTTGTTCCACATGGAG---CAAGAAAACCATTATTTGGAACAAATCCAATTG
3           CTCTATATCTTCTTTCTCCTGGCATTCTTGTTAATCCAACTGCTTGCATATGTTCAACTA
plasmid     TGACATGTGTTGTTCCACATGGAG---CAAGAAAACCATTATTTGGAACAAATCCAATTG

1           -ATTAGGAGT------TGAAATGAATGAATTTGTTATGACAGATGATAATACATTTTATT
2           CATTTGCAGCACCATGTGCAGAACATGATCCAATTGTTTTTGATATGGCAACATCTGCAA
3           ATTCTCTAGATCTTTGTGCAAATCTTTGTCCTTCTGCTTTTCCTGGATCAATAACAATAA
plasmid     CATTTGCAGCACCATGTGCAGAACATGATCCAATTGTTTTTGATATGGCAACATCTGCAA

1           TAGTTAATGGAGTTAGAGAAAG---AACATATGTTGTTCAAGAAAATCCAGATGTTTTAA
2           TGGCACATGGAGATGTTCAAATTGCAGCAAGAGCAGGACAACAATTACCAGAAGGAATGG
3           TTAATTGTCCTGTCCATGGTGTTTTTGCTCCTGGATGTCCAGACCAATCAAATTCCCAAG
plasmid     TGGCACATGGAGATGTTCAAATTGCAGCAAGAGCAGGACAACAATTACCAGAAGGAATGG
```

Figure C.3: Sequencing results for positive pBV2xp-*aip*^{SjBi}-*dpkA*^{Pp}. Part 1. 1, 2, and 3 indicates the different sequencign results, while plasmid is the theoretical plasmid.

Figure C.4: Sequencing results for positive pBV2xp-aip^{SjBi}-$dpkA^{Pp}$. Part 2. 1, 2, and 3 indicates the different sequencign results, while plasmid is the theoretical plasmid.

The sequencing results shown in Figure C.3 and Figure C.4 shows that pBV2xp-aip^{SjBi}-$dpkA^{Ps}$ has been constructed correctly.

D Raw data

Due to the large amount of raw data, the raw data was omitted from the report. The raw data can be obtained on request, contact bskagestad@yahoo.no.

E Calculation

E.1 Growth rates

In order to calculate the growth rate of a particular bacterial culture, first, the $\log(OD_{600})$ of that particular culture was plotted against time. Then, all of the data points not appearing in a linear line on the graph were discarded, and an exponential regression was performed on the data, and the growth rate of the culture will be the factor in front of the exponent or b in Equation E.1.

$$f(x) = a \cdot e^{b \cdot x} \tag{E.1}$$

E.2 Obtaining concentrations in samples from the HPLC utilizing standard curves

In order to obtain the concentrations of the different samples from the HPLC, first, the known concentrations of the standards have to be plotted against their absorbance to create a standard curve. Then a linear regression was applied to get a relation between absorbance and concentration of the amino acid in question. After this is done, the relation can be applied to the raw data to calculate the unknown concentrations of the samples.

E.3 Standard deviation

The standard deviation is a measurement indicating the uncertainty in a data set. The measure describes the spread of the data (variance) obtained under similar conditions. In this study, the standard deviations were calculated using the "STDAV.P" function in Microsoft 365 Excel.

F List of primers

Table F.1: List of primers utilized in present study

Primer name	Sequence (5'-3')	Description
aipTvcodopt2fw	CTTGTTCACTTAAGGGGGAAATGGCTAT GGATAATGTTGATTTTGCAGAATCTG	Forward amplification of *aipTv* for pBV2xp-aip^{Tv}-$dpkA^{Ps}$
aipTvcodopt2rv	GTTGGTTGATCTGCATGAGATGCAGACA TGTACTACTACCTCCTATTTATGTAAT TGTTTATTAAATTTTAACTTGATAT TCTTTTGG	Reverse amplification of *aipTv* for pBV2xp-aip^{Tv}-$dpkA^{Ps}$
dpkaPsfw	AAAAGAATATCAAGTTAAAATTTAATAAA CAATTACATAAATAGGAGGTAGTAGTA-CATG TCTGCATCTCATGCAGATCAAC	Forward amplification of $dpkA^{Ps}$ for pBV2xp-aip^{Tv}-$dpkA^{Ps}$
dpkaPsrv	GCCAGTGAATTCGAGCTCATGGTACGGAT CTTAATGTCCTGCTAATTCTTGTAATC	Reverse amplification of $dpkA^{Ps}$ for pBV2xp-aip^{Tv}-$dpkA^{Ps}$
aipSjcodopt2fw	CTTGTTCACTTAAGGGGGAAATGGCT	Forward amplification of *aipSjBi* for pBV2xp-aip^{SjBi}-$dpkA^{Ps}$
aipSjcodopt2rv	GTTGGTTGATCTGCATGAGATGCAGA CATGTACTACTACCTCCTATTTATGTA ATTGTTTATTAAATTTTAACTTGATATT CTTTTGG	Reverse amplification of *aipSjBi* for pBV2xp-aip^{SjBi}-$dpkA^{Ps}$
dpkaPs2fw	CTACAATTGAACATACAAAAGATGAATTA TAATAAACAATTACATAAATAGGAGGTAG TAGTACATGTCTGCATCTCATGCAGAT CAAC	Forward amplification of $dpkA^{Ps}$ for pBV2xp-aip^{SjBi}-$dpkA^{Ps}$
dpkaPs2rv	GCCAGTGAATTCGAGCTCATGGTACGG ATC	Forward amplification of $dpkA^{Ps}$ for pBV2xp-aip^{SjBi}-$dpkA^{Ps}$
aipSjcodopt3fw	CTTGTTCACTTAAGGGGGAAATGG CTATGGAACATTTAGCAGATTGTTT AGAAGATAAAG	Forward amplification of *aipSjBi* for pBV2xp-aip^{SjBi}-$dpkA^{Pp}$
aipSjcodopt3rv	GATTGTAATTCTGTAAATGGAACTCTCATG TACTACTACCTCCTATTTATGTAATTGT TTATTATAATTCATCTTTTGTATGTTC AATTG	Reverse amplification of *aipSjBi* for pBV2xp-aip^{SjBi}-$dpkA^{Pp}$
dpkaPp2fw	CAATTGAACATACAAAAGATGAATTATAAT AAACAATTACATAAATAGGAGGTAGTAG TACATGAGAGTTCCATTTACAGAATTA CAATC	Forward amplification of $dpkA^{Pp}$ for pBV2xp-aip^{SjBi}-$dpkA^{Pp}$
dpkaPp2rv	GCCAGTGAATTCGAGCTCATGGTACGGA TCTATCCTAATAATTCTTTTAATCCTTT-TAATTC	Reverse amplification of $dpkA^{Pp}$ for pBV2xp-aip^{SjBi}-$dpkA^{Pp}$
pxpf	TGTTTATCCACCGAACTAAG	Forward primer utilized to amplify region downstream of the xylose promoter in pBV2xp
bvxr	CCGCACAGATGCGTAAGGAG	Reverse primer utilized to amplify region downstream of the xylose promoter in pBV2xp

G DNA Ladder

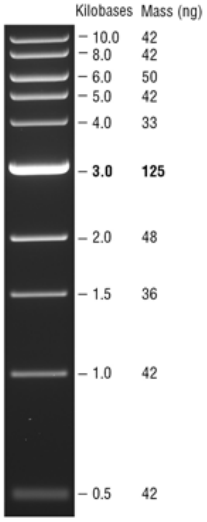

Figure G.1: NEB 1 kb DNA Ladder utilized under gel electrophoresis in study. [47]

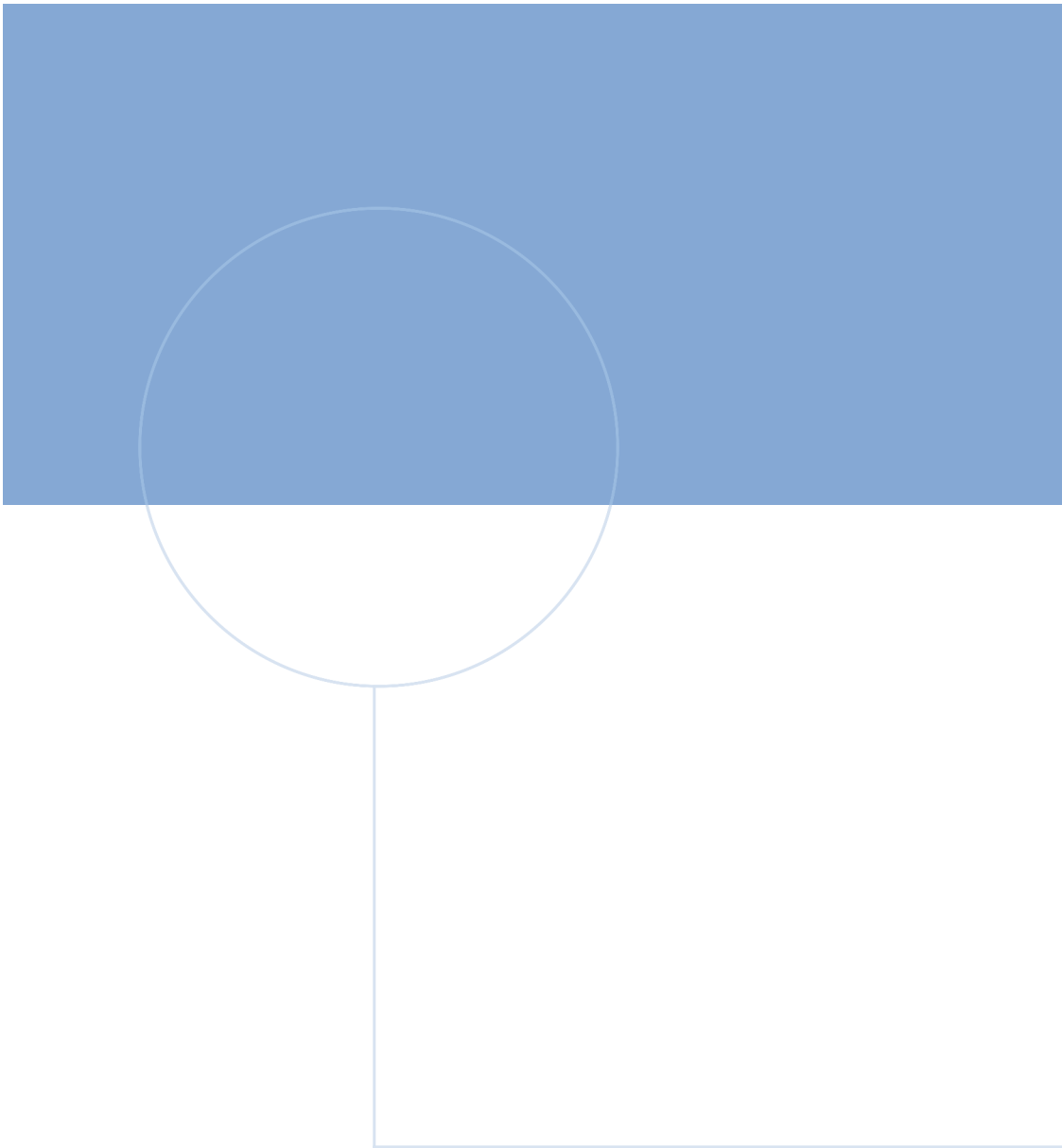

NTNU

Norwegian University of
Science and Technology